ARPA ORDER NO. 189-1

MEMORANDUM
RM-5506-ARPA
JULY 1968

EXPLORATORY STUDIES ON THE SUBLIMATION OF SLENDER CAMPHOR AND NAPHTHALENE MODELS IN A SUPERSONIC WIND-TUNNEL

A. F. Charwat

PREPARED FOR:
ADVANCED RESEARCH PROJECTS AGENCY

The RAND Corporation
SANTA MONICA • CALIFORNIA

ARPA ORDER NO. 189-1

MEMORANDUM

RM-5506-ARPA

JULY 1968

EXPLORATORY STUDIES ON THE SUBLIMATION OF SLENDER CAMPHOR AND NAPHTHALENE MODELS IN A SUPERSONIC WIND-TUNNEL

A. F. Charwat

This research is supported by the Advanced Research Projects Agency under Contract No. DAHC15 67 C 0111. RAND Memoranda are subject to critical review procedures at the research department and corporate levels. Views and conclusions expressed herein are nevertheless the primary responsibility of the author, and should not be interpreted as representing the official opinion or policy of ARPA or of The RAND Corporation.

The RAND Corporation

PREFACE

Past studies of sublimation during reentry were mostly concerned with blunt bodies and situations in which there was relatively little total erosion. Recent developments have focused on problems associated with the behavior of slender reentry bodies in which the profile of the vehicle, and particularly that of the tip, can change substantially during flight. For example, even relatively shallow ablation patterns etched into the vehicle surface can affect vehicle performance. It may eventually become possible to design ablating surfaces which erode substantially during reentry, allowing us to program the drag history of the vehicle's trajectory. To investigate such problems, it is necessary to conduct wind-tunnel tests under closely controlled and reproducible conditions. The exploratory tests described herein include:

a. the development of a method of preparing camphor and naphthalene, which are convenient materials for fundamental studies of aerodynamic sublimation, and
b. a series of experiments with simple and complex conical shapes having forward- and downstream-facing steps, notches, and shoulders.

Their purpose was to identify the general features of the problem and to evaluate the potentialities of this experimental technique. On all counts, the tests suggest the desirability of systematic quantitative tests and a simultaneous analytical effort.

The author, A. F. Charwat, is a professor in the Department of Engineering at the University of California, Los Angeles, and a consultant to The RAND Corporation.

SUMMARY

A method of sintering powdered camphor and naphthalene after deaeration under vacuum is described. It is shown that models machined out of stock prepared in this way have a shear strength twice that of cast models, are completely homogeneous, and are well suited to wind-tunnel experiments on the aerodynamics of subliming bodies. At a Mach number of three and an overall free stream Reynolds number of 3×10^5, exploratory tests were performed on cones with flat and hemispherical noses and on several complex conical shapes prepared in this manner, and featuring downstream and upstream facing steps, rectangular grooves, and shoulders. The results are described, emphasis being placed on the general evolution of their profiles, the sublimation history of the tips, and the occurrence of grooves, striations, and surface markings. A suggestive generalization from these observations is that ablation patterns are extremely sensitive to vortical disturbances in a boundary layer, which in the absence of mass transfer is decidedly laminar.

CONTENTS

PREFACE iii

SUMMARY v

Section
I. INTRODUCTION 1

II. PROPERTIES OF CAMPHOR AND NAPHTHALENE 3
Casting Problems 6

III. EXPERIMENTAL FACILITY AND TECHNIQUE 10

IV. EXPLORATORY RESULTS 13
Sublimation of a Blunted Cone -- Influence of the Tip 13
Ablation of Bodies with Regions of Separated Flow 24

V. DISCUSSION 35

VI. CONCLUSIONS 43

Appendix
A. AEROTHERMODYNAMICS OF AIR/CAMPHOR AND AIR/NAPHTHALENE SYSTEMS 45

B. TECHNIQUES OF CASTING AND SINTERING THE MODELS 55
Recrystallized Models: Casting and Testing 55
Dip Casting (Layer Recrystallization) 56
Open-Air Sintering (Undeaerated) 56
Deaerated Powder Sintering 57

REFERENCES 65

I. INTRODUCTION

Past work on the development of ablative heat shields for reentry vehicles was dominated by thermal and structural problems, and focused mainly on applications to blunt bodies. In these applications a relatively thin shell of material ablates without influencing the geometry or the aerodynamic characteristics of the vehicle. However, the recent emphasis on low-fineness-ratio cones has given prominence to the importance of changes in shape of the ablating surface, particularly in the neighborhood of the nose. These changes can seriously affect the drag, the aerodynamic stability parameters of the vehicle, and the aerothermochemical conditions which influence the mass and composition of observables left in the wake of the body.

Recent experiments[1-4] have brought to light some fine details of the surface features left on the ablated skin after flight, which are of considerable fundamental interest. These include streamwise grooves sometimes associated with identifiable three-dimensional roughness elements. The grooves are obviously related to vortex patterns formed behind disturbances in the boundary layer, and are often referred to as "turbulence wedges," but it is not certain whether they are indeed associated with a true laminar/turbulent transition. An even more surprising pattern, only recently identified, looks like "cross-hatching" produced by grooves spiraling in both directions over the surface. The conditions under which they occur are not clear. They have been observed on several recovered reentry nose cones, on models tested in ballistic ranges, and in the wind tunnel on cones with various half-angles.*

A characteristic of the coupling between an ablative surface and the flow in the boundary layer is that only certain disturbances become "frozen in." Similarly, some features of the geometry of complex (composite) initial shapes with corners, steps, etc., are eroded smoothly

*The existence of such striations has been associated experimentally with supersonic transitional or turbulent flow over the body surface.

and stably, whereas others tend to magnify or induce further self-perpetuating nonuniformities. There have been virtually no papers published on such phenomena or on the possible uses of the coupling between the trajectory and the history of shape/drag/ablation thermochemistry of such composite shapes.

One of the difficulties in experimental research in this field stems from the need for facilities with a high stagnation enthalpy, even for the testing of practical "low-temperature" ablators. The complexity of the theoretical aerothermochemical problem, the difficulty of formulating scaling laws, and the emphasis on testing materials for practical applications have all contributed in the past to a resistance to the use of substitute materials which change phase at reasonably low temperatures. Although some work with camphor, naphthalene, dry ice, water ice, etc. has been reported,[5,6] the use of these materials has never been fully explored. Concern with the new fundamental aerodynamical aspects of the problem and their relation to the history of the body shape suggests that "duplication" of thermochemistry may now become less essential than the ability to observe and to measure in detail, and that one should reconsider model tests using artificial but convenient test materials.

The present report summarizes a systematic study of the preparation and use of camphor and naphthalene for wind-tunnel investigations of the aerodynamics of ablating bodies, and describes exploratory results on the surface-recession history of cones, blunted cones, and composite shapes having expansion corners, upstream and downstream flow separations, and notches. The experiments were performed by the author over a period of three years[7] at U.C.L.A. with the assistance of several students,[8] but without specific funding. As a consequence of limited resources, the amount and precision of the photographic records and auxiliary measurements are not sufficient to allow a detailed and quantitative reduction of data and a comparison with theory. As an exploratory program, however, the tests were quite successful, and further exploitation of the possibilities of the techniques developed as well as the study of the ablation of bodies more complex than those described below, seems quite worthwhile.

II. PROPERTIES OF CAMPHOR AND NAPHTHALENE

There is a small number of readily available substances that sublimate or ablate in a fashion that can be described fairly accurately by theory at temperatures low enough to make instrumentation and measurements convenient. Foremost among them are dry ice, camphor, and naphthalene. Among other materials considered in the literature are hexachloroethane, chloronil, and ammonium cnloride. Both camphor and naphthalene have been used to a limited extent. They are easy to handle, and at first sight their range of thermochemical phase change appears to be extremely convenient for use at reasonable supersonic Mach numbers in continuous wind tunnels.

A brief summary of basic physical constants of naphthalene and camphor is given in Table 1. A phase diagram of the pure forms of these substances in the low-pressure region is shown in Fig. 1 and compared to some typical pressure in a wind tunnel operating at atmospheric stagnatic conditions (Mach number 3). (There is some disagreement in the handbook literature relating to the physical constants, partly because of differences in the physical properties of the samples.)

The superposition of the partial equilibrium pressures of phase change and the wind-tunnel pressures does not yield a direct comparison; these pressures are related by the magnitude of the local blowing parameter, and thus depend on the solution of the binary boundary-layer problem. Using a simple form of sublimation theory, we have calculated the variation of the blowing parameter, the Stanton number, and the ablation rate for a flat plate boundary layer in a camphor-air and naphthalene-air system; the results are presented in Appendix A. It is seen that in an easily accessible range of wind-tunnel conditions with stagnation temperatures between room temperature and $1000^{\circ}F$ and static pressures corresponding to reasonable Mach numbers attained from stagnation pressures of the order of one atmosphere, one can obtain a complete range of blowing parameters with pure sublimation (solid/gas transition without a liquid phase change). Camphor is virtually always below the triple point, whereas naphthalene,

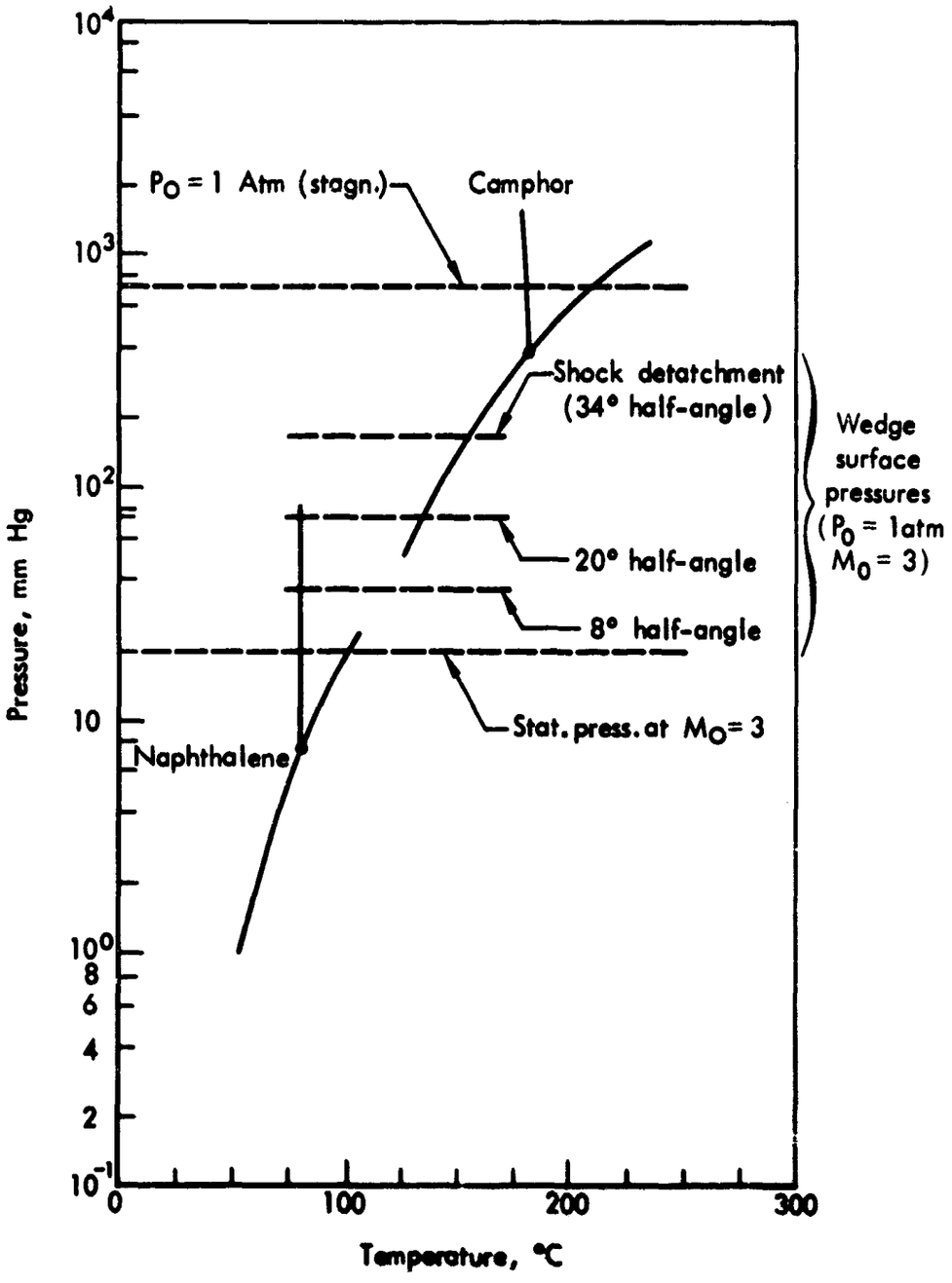

Fig. 1—Equilibrium phase diagrams of camphor and naphthalene relative to typical pressures in an atmospheric-stagnation-pressure tunnel, M = 3

Table 1

APPROXIMATE BASIC PHYSICAL PROPERTIES OF CAMPHOR AND NAPHTHALENE

Property	Substance	
	Camphor (d-)	Naphthalene
Formula	$C_{10}H_{16}O$	$C_{10}H_8$
Molecular weight	152.23	128.1o
Crystalline form	hexagonal	monoclinic
Density (solid) (gr/ml)	0.99 (62.4 lb/ft^3)	1.145 (71.5 lb/ft^3)
Normal boiling temp. (^oC)	204 (399^oF)	217.9 (436^oF)
Normal melting temp. (^oC)	176-177 (355^oF)	80.22 (176.5^oF)
Triple point: T_{TP}(^oC)	180.1	80.1
P_{TP}(mm Hg)	385.8	7.50
Heat of sublimation (cal/gr)	58.5 (105.7 Btu/lb)	138 (237.5 Btu/lb)
Heat capacity (solid) (cal/gr^oC)	0.445	0.285
Heat capacity (gas) (cal/gr^oC)	.283	.266
Heat capacity (liquid) (cal/gr^oC)	.440	.424
Thermal conductivity (solid) (cal/cm sec ^oK)	0.96×10^{-3} (2.7×10^{-6} Btu/in.-sec ^oF)	1.8×10^{-3} (5.05×10^{-6} Btu/in.-sec ^oF)

for which the triple-point pressure is an order of magnitude below that of camphor, can be made to undergo melting ablation at very high blowing rates. Parenthetically, one might mention that camphor vapors are highly flammable, and combustion in the boundary layer seems to be sustainable (possibly by increasing the oxygen content of the wind-tunnel air).

CASTING PROBLEMS

Both camphor and naphthalene are anisotropic crystalline materials. Early experiments indicated that the development of a technique for casting sufficiently homogeneous models constitutes the key to a successful use of these materials for wind-tunnel testing. In all previous experiments known to the author, models were prepared either by direct casting at high (atmospheric) pressure or by layer casting (dipping) of a basic core in liquid material. The stock so produced is subsequently machined or sanded to the desired shape. Upon trying this technique we found it entirely unsatisfactory, especially for making small models with a high fineness ratio. (In Appendix B we review our experience with various methods of casting.) By a process of elimination, we concluded that our difficulties arose from:

a. the crystalline nature of the castings, and
b. the loosening of the intercrystalline bond as the result of adsorption of inert gases (air) at the surface of the successive layers of material, the gas being contained in microscopic voids in the body of the model.

To solve this problem, we developed a technique for casting stock cylinders whereby the powdered material is placed in a special mold equipped with pistons; it is then subjected to a vacuum that causes it to sublimate, releasing the entrapped gases, which are then expelled from the mold by a pump, and the material is subsequently sintered by compression (see Appendix B). A photograph of a stock cylinder 2 inches long and 1/2 inch in diameter immediately after fabrication is shown in Fig. 2. The material is translucent, and within an

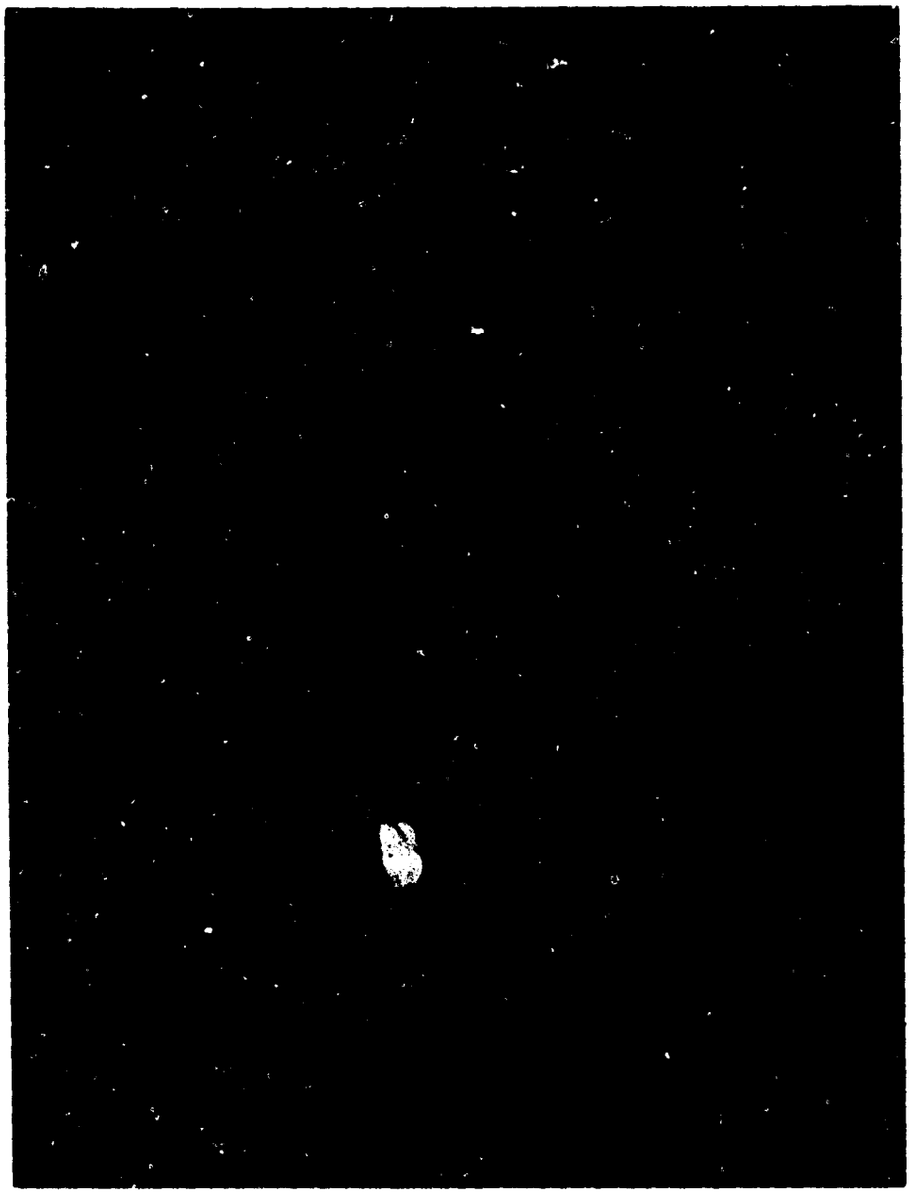

Fig. 2—Typical stock-cylinder of vacuum-sintered camphor (2.5 inches long, 0.6 inches in diameter)

hour after sintering at room temperature becomes completely transparent. This final curing results from internal relaxation of the material's microcrystalline structure and its absorption of whatever camphor vapor might have been trapped in microvoids during sintering.

It is intuitively clear that a homogeneous, transparent model will be preferable for wind tunnel testing to models that are visibly crystalline in nature, opaque, and full of stress lines (resembling moth balls). Repeated testing of standard (7-1/2-deg half-angle) cones in the tunnel verified that sintered models yield many more reliable and reproducible data than models made by other casting techniques. With sintered models we observed no breaking at the tip or shearing off of chunks of material, as occurs with cast models, which also often exhibit patches of surface with properties markedly different from those of neighboring patches (often distinguishable visually by a difference in color or texture).

One of the control tests performed during these experiments consisted of measuring the shear stress and the density of sample cylinders. Cast and dipped models of camphor yielded shear stresses between 64 and 72 psi, whereas sintered models exhibited a shear strength between 100 and 125 psi. Similarly, naphthalene models supported a shear stress of 55 psi when cast and 160 psi when sintered. The density of cast models (both camphor and naphthalene) was consistently lower (between 3 and 8 percent) than that of sintered models. The method finally adopted was to vacuum-deaerate the camphor or naphthalene powder for 15 minutes at room temperature and then sinter it by compression to 4000 psi. Camphor and naphthalene samples treated in this way had densities of 63.4 and 73.5 lb per cubic foot, respectively [which are actually somewhat higher than most handbook values (see Table 1)].

The wind-tunnel models were machined out of stock cylinders such as those shown in Fig. 2. The material machines easily; its surface is smooth and slightly oily to the touch, although it is somewhat brittle; we found it difficult, for example, to machine the nose down to a sharp point without using a special tool. We feel, however, that this offers no great difficulty should it be desirable.

Camphor is slightly easier to sinter than naphthalene, and results in a more nearly transparent stock -- possibly because naphthalene is composed of leaflet-shaped particles, which are less suited to compression sintering than the hexagonal crystals of camphor. In the wind tunnel, however, naphthalene models behave fully as satisfactorily as camphor models produced by this technique.

Preliminary experiments to measure the specific heat and the latent heat of sublimation of the sintered stock were made, but current results are not precise enough to warrant publication. Suffice it to say that they are within 10 percent of the handbook values.

III. EXPERIMENTAL FACILITY AND TECHNIQUE

The wind tunnel used is a sliding-block type with a variable Mach number, and has a test section measuring 3 by 3.5 inches. Atmospheric air is admitted through a silica-gel dryer and a stainless-steel heat exchanger operated on a natural-gas burner. The present exploratory data were obtained at two Mach numbers, M = 2.78 and M = 3.05, and at stagnation temperatures varying between 70 and 180°F. The experiment will be extended to the full range of the tunnel's test conditions (Mach numbers between 1.5 and 4.5 and stagnation temperatures up to 1000°F) after the experimental setup is modified in certain minor respects, which will include a mechanism allowing the model to be swung into the test section after the flow is established.

The model is sting-mounted on a variable-angle-of-attack quadrant affixed to the wind-tunnel wall. At present, it takes about ten seconds to insert a model, close the diffusor, and start the tunnel, and another eight seconds to establish the flow (as measured by a stagnation thermocouple in the test section). These delays are of no essential consequence at the relatively low stagnation temperatures reported here (which correspond to blowing parameters between .05 and .15 -- see Appendix A).

The free-stream Reynolds number in the test section was approximately 1.5×10^5 per inch. The models were initially two inches long. It follows that the boundary layer was laminar over the entire model (except in the neighborhood of specific macroscopic disturbances at the surface).

The sliding-block design of this wind tunnel represents a compromise in nozzle contours that results in a slight nonuniformity in the flow at all Mach numbers. At the present settings the Mach number over the region occupied by the model is quite constant, varying (streamwise) by less than one percent. However, the direction of the free stream varies somewhat. Calibrations in the empty tunnel using a four-orifice, spherical-nose yaw probe showed a directional nonuniformity of about one deg over the cross section with a velocity distribution changing with nozzle setting. This is the reason for testing

at two neighboring settings, M = 2.8 and 3.05, which exhibited opposing deviations from the mean. Observations of the surface recession, including the appearance of scars and grooves, showed no differences between these settings; it was thus concluded that the slight nonuniformity in free-stream direction was inconsequential within the overall accuracy of the results.

Records of the model profile were obtained by photographing with a 16-mm camera the shadow projected by the body in the parallel light of the Schlieren system on a graduated translucent screen. Still photographs of the model in the wind tunnel were obtained, as well as some photographs taken through the Schlieren optics. A time base was provided by a stop-watch in view of the camera, and the free-stream temperature and impact pressures were continuously recorded. These records are qualitatively good, but for the relatively coarse-grained (Tri-X) film used, the 16-mm frame size proved too small to allow an accurate reduction of data on the surface-recession rate (which was of the order of a few ten thousands of an inch per second on the afterbodies under prevailing test conditions).

Concurrently with these experiments, a technique for measuring the local surface temperature of the model was developed, but has not yet been applied in the wind tunnel. The technique makes use of the temperature sensitivity of the spectral distribution of photoluminescence of certain materials. A quantity of fluorescent powder (typically 5 percent by weight) is mixed with the camphor or naphthalene powder before sintering. When irradiated by an ultraviolet source (the mercury lamp of the Schlieren system), the model glows faintly. A focused optical system receives the light emitted by an element of surface (about one mm square) and views it by two photomultiplier cells through two different filters. The relative intensity of the light recorded by the cells and measured differentially on a bridge is an indication of the color and local surface temperature (independent of the intensity of the exciting irradiation or the local density of the fluorescent material in the model). The system was successfuly bench calibrated using Radelin 1807 (ZnCdS:Ag,Ni), Sylvania 140 (ZnCdS:Ag)

and other fluorescent powders as indicators and 520- and 590-Angstrom (8-millimicron half-bandwidth) filters. The present instrument typically yielded bridge imbalances of .14 mv per degree F in the range of 50 to 200°F. The relation is fairly linear, with sensitivity and range dependent on the material. On the other hand, since the fluorescent material was found to age over periods of the order of one day, the instrument could not be calibrated absolutely.

IV. EXPLORATORY RESULTS

SUBLIMATION OF A BLUNTED CONE -- INFLUENCE OF THE TIP

Figure 3 shows a sequence of Schlieren photographs of a subliming camphor cone with a hemispherical nose. Figure 4 shows a similar test, except that the nose of the cone was initially flat (both cones having the same initial diameters). The blowing parameter $B' = \dot{m}/\rho_e u_e C_H$ corresponding to these test conditions is approximately .035 (see Appendix A).

A remarkable feature of these records is the sharpening of the nose to a point. Although the body becomes blunter as it sublimates, in the sense that the overall fineness ratio decreases, the tip becomes sharp. This occurs whether the initial slope is continuous (hemispherical) or discontinuous (flat). The afterbody sublimates initially to a slightly concave profile immediately downstream of the nose shoulder, indicating a higher heat-transfer rate in that region. As the nose shape sharpens and stabilizes, the afterbody assumes a convex power-law profile.

Figure 5 shows two still photographs of a similar model at 30-second intervals (approximately 3 minutes after the beginning of the test) in the wind tunnel at a higher Mach number ($M = 3.05$) and at a stagnation temperature of $140^{\circ}F$, which now corresponds to a blowing parameter of $B' = .12$. The tip is even sharper at this blowing rate, and tends to form a very fine point. The second photograph shows the development of streamwise grooves, which originate at the needle tip as it breaks off somewhat nonuniformly.

Figures 6 and 7 show two studies of naphthalene cones with flat tips .1 and .25 inches in diameter, respectively. The stagnation temperatures are higher, so that the blowing parameters B' for this material are in the same range as those for the first camphor model ($B' = .055$ and $.035$, respectively). The recession histories of the tips are nonetheless obviously different, as the naphthalene models retain a definite hemispherical nose shape.

Existing analyses shed no light on this pronounced qualitative difference in the tip behavior of camphor versus naphthalene models.

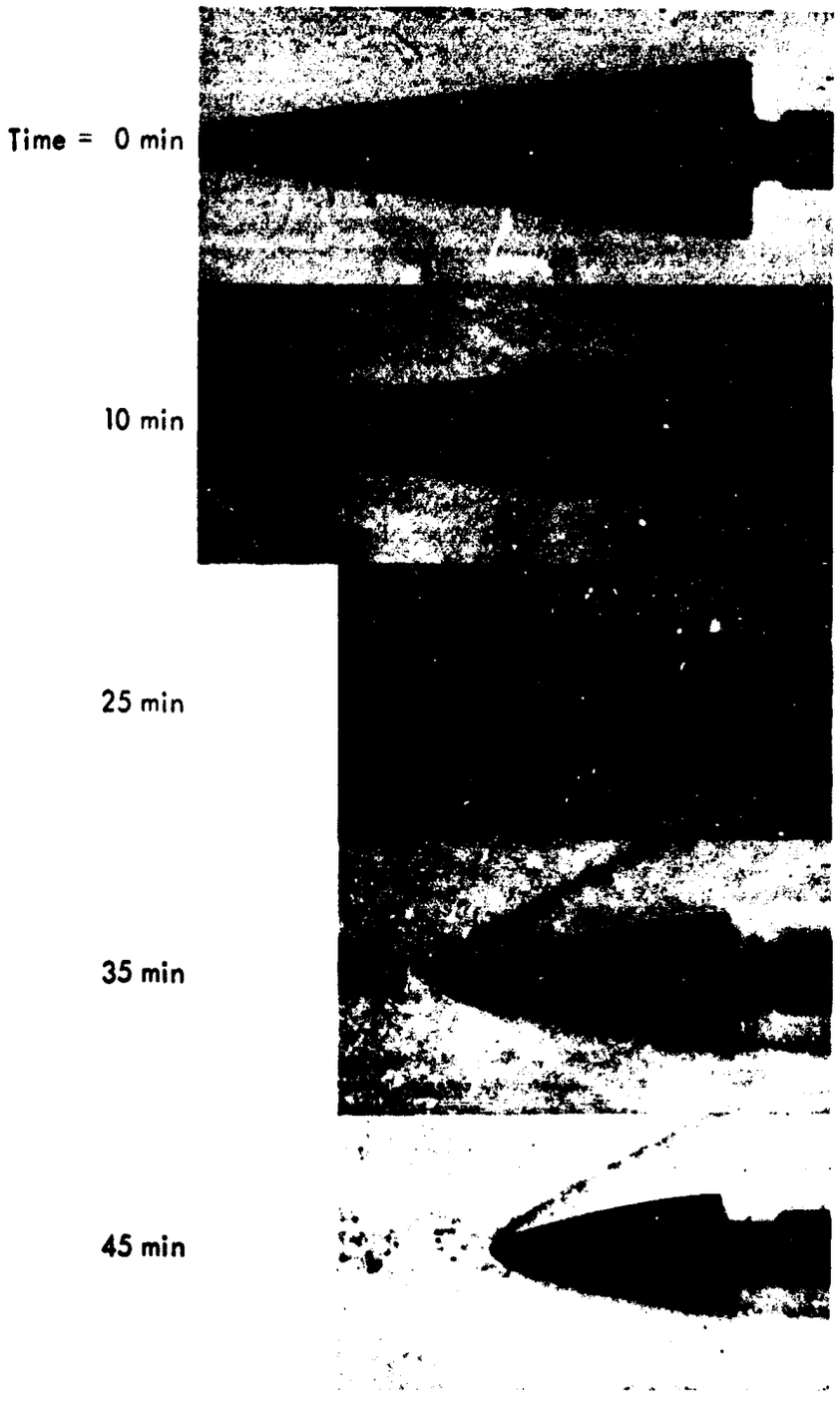

Fig. 3—Sublimation of a blunted cone (hemispherical nose): camphor, $M = 2.78$, $T_0 = 80^0$ F, $P_0 = 1$ atm

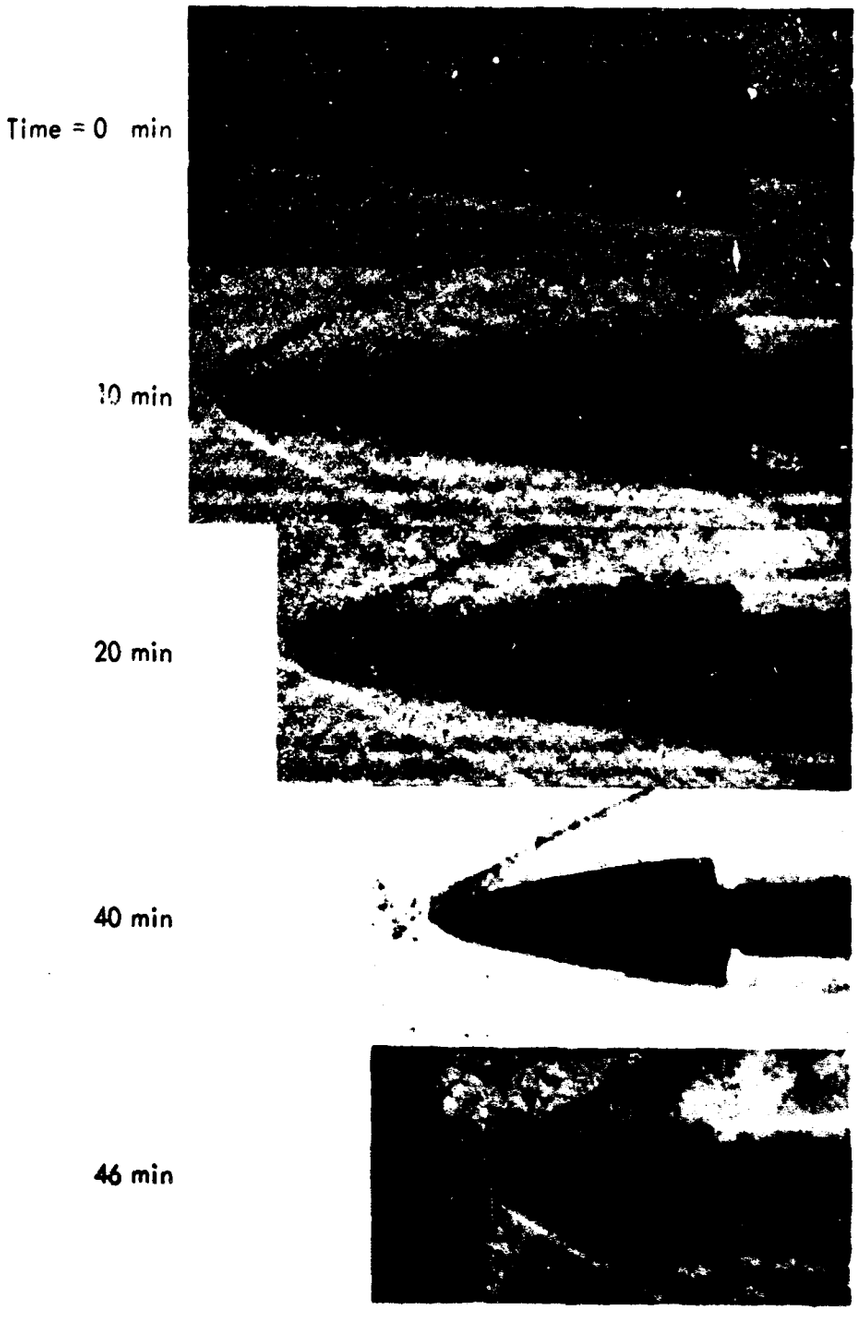

Fig. 4—Sublimation of a blunted cone (flat nose): camphor, $M = 2.78$, $P_0 = 1$ atm, $T_0 = 80°F$

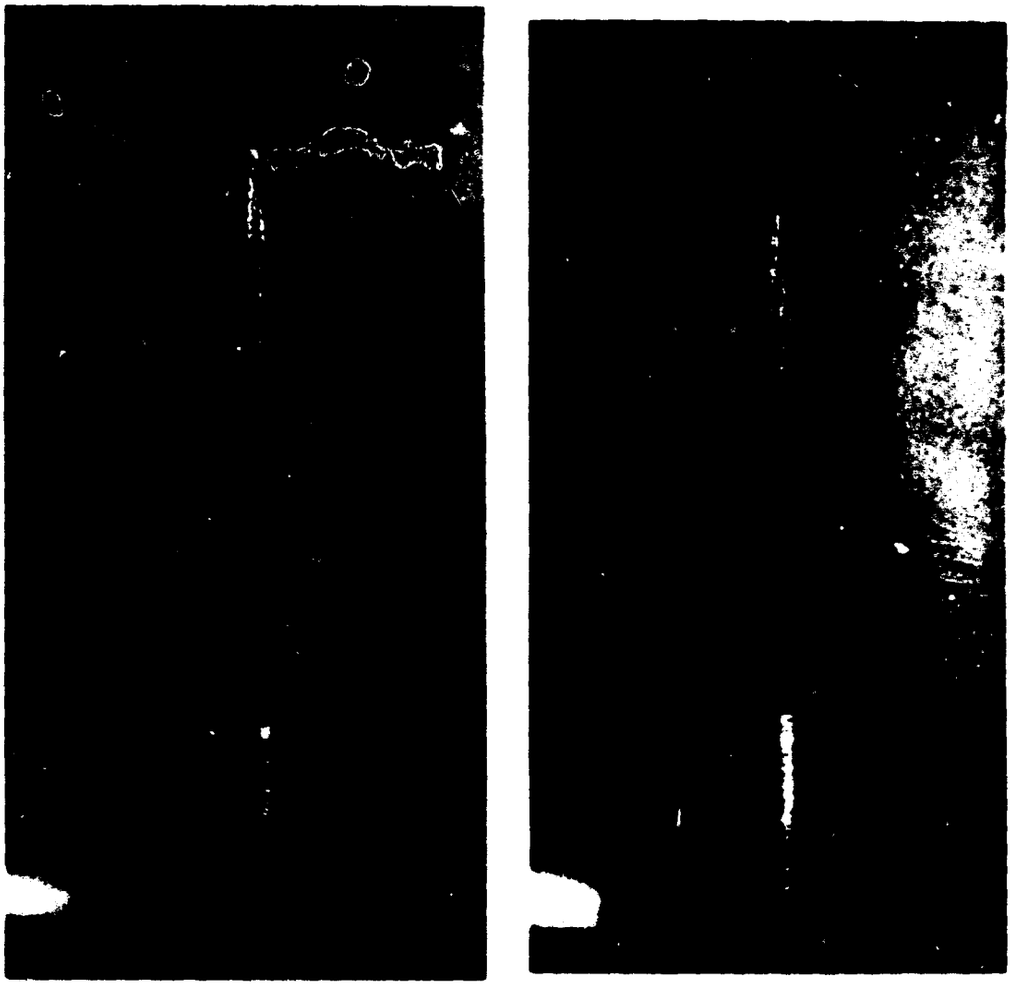

Time = ~3 min ~3 min 30 sec

Fig. 5—Photographs of a flat-nosed cone in wind tunnel after 3 and 3.5 minutes; camphor, M = 3.05, P_0 = 734.6 mm Hg, T_0 = 140°F

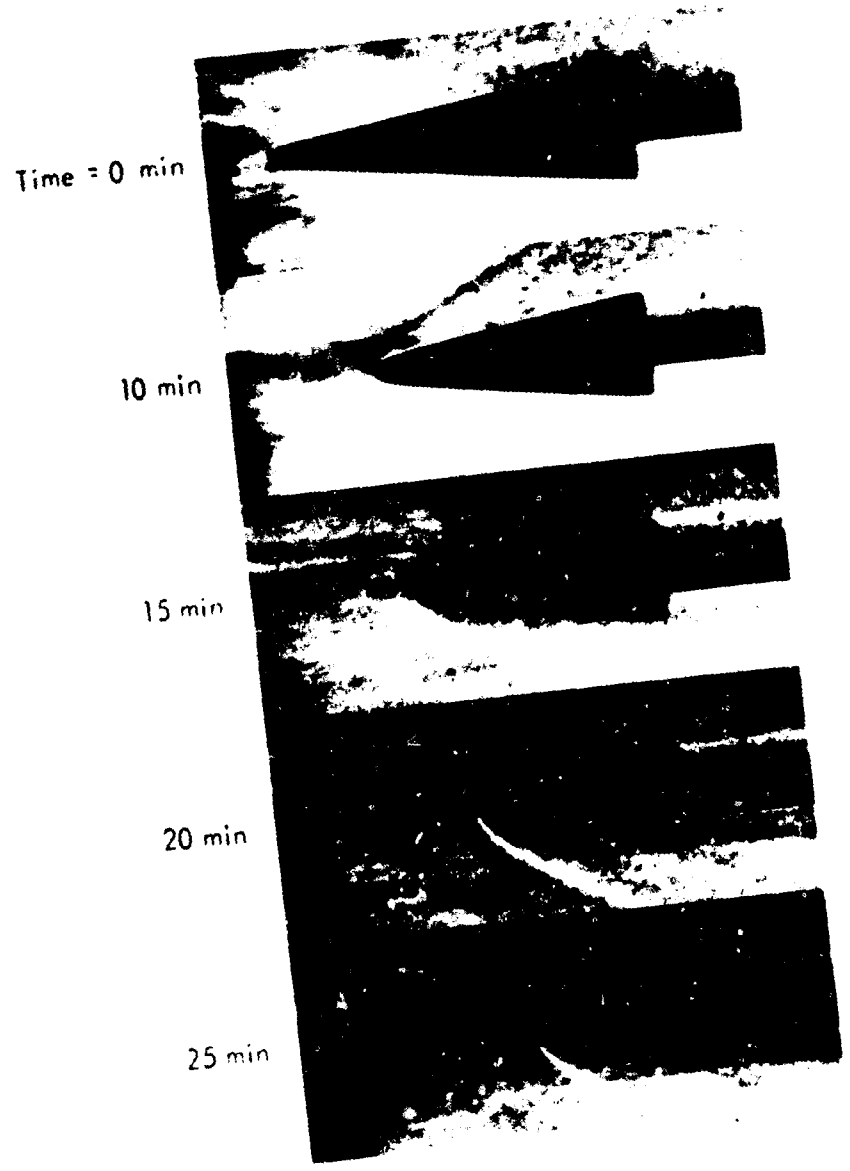

Fig. 6--Sublimation of a blunted cone (flat nose); naphthalene. $M = 2.78$, $P_0 = 1$ atm, $T_0 = 164^0$ F

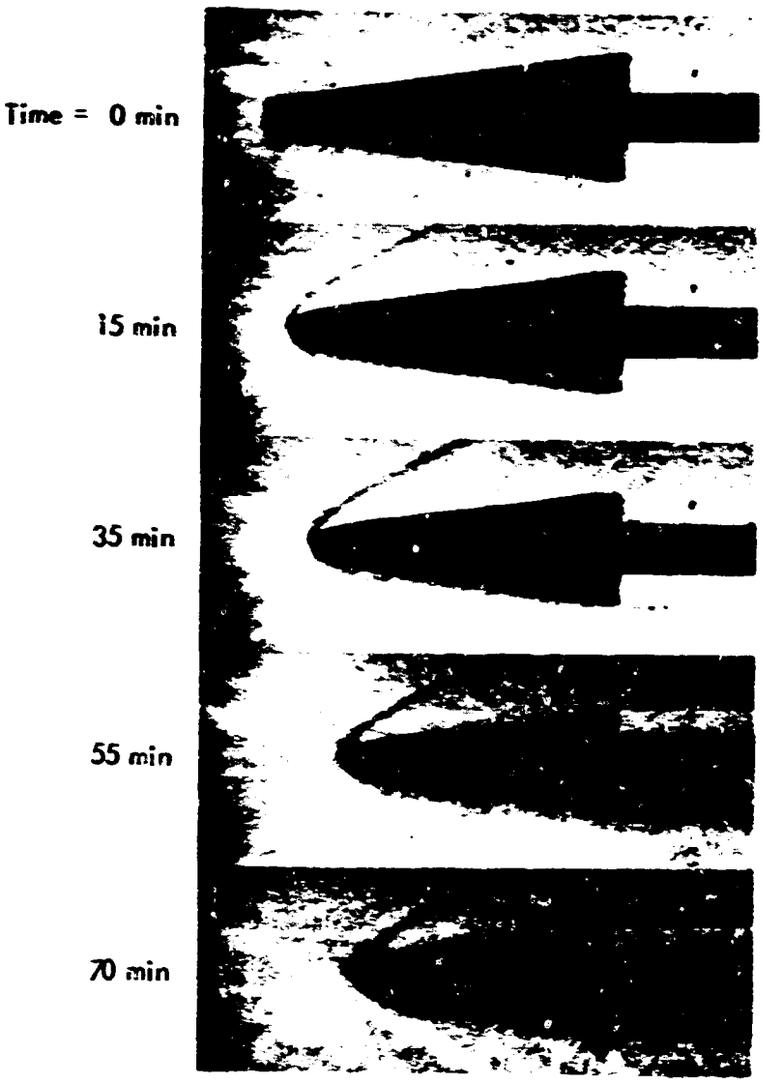

Fig. 7--Sublimation of a blunted cone (flat nose); naphthalene, M = 2.78, P_0 = 1 atm, T_0 = 137°F

We know of one other laboratory study which reported the sublimation of models (graphite cylinders[10]) to a needle-point tip as sharp as those we observed. Laminar/turbulent transition, which is sometimes identified as the cause of erosion that sharpens the shoulder of a blunt nose, obviously does not occur here. We feel that an adequate theory of this behavior must account for (1) the integral nature of the problem (i.e., that the shape at any instant depends on the entire previous history); (2) the phase-change kinetic contraints on the process of sublimation in the region of the tip (see Ref. 9); and (3) two-dimensional, unsteady heat conduction under the ablating surface.

Figures 8 and 9 show, respectively, the evolution of the profile of a flat-nosed camphor cone at a 5-deg angle of attack, traced from enlarged film records, and still photographs of the same cone taken through the wind-tunnel wall. The tip of the model behaves the same as at zero incidence. The grooves originate at the tip, and in one case, somewhat downstream of the tip (see photograph at 125 sec), and spiral from the windward to the lee side of the yawed cone. The photographs show traces of camphor powder recondensed both on the lee side of the body and in the base wake of the model.

Figures 10 and 11 show similar data for a 25-deg cone with a cylindrical afterbody at zero incidence. This sequence exhibits an interesting regular pattern of streamwise grooves on the forebody; the grooves do <u>not</u> originate from the tip. Moreover, the relatively pronounced concavity of the profile (see photograph at 125 sec) suggests that the forebody striations are associated with the formation of a Görtler vortex pattern. The order of magnitude of their spacing sustains this interpretation. (Similar markings are discussed below in connection with the downstream-facing step, which also results in a basically convex body profile.) The convexity of this model is associated with the nose sublimation history discussed previously.

The expansion corner sublimates to a smooth curve of gradually increasing radius of curvature. Theoretical analysis of the recession history of such a corner requires that two-dimensional internal heat transfer be taken into account.

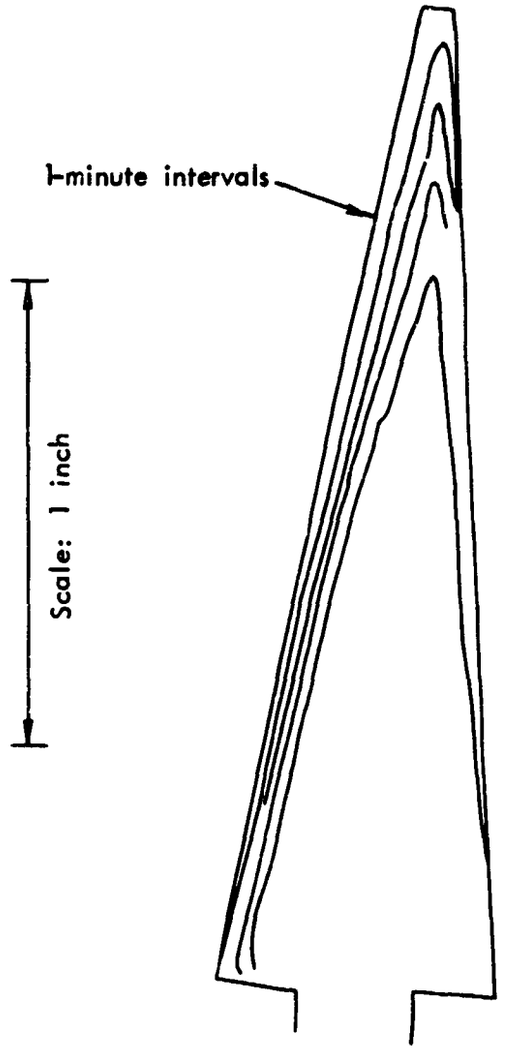

Fig. 8—Profiles of a flat-nosed, 15-degree cone at incidence of 5 degrees at 1-minute intervals; camphor, $M = 3.05$, $P_0 = 735$ mm Hg, $T_0 = 141°$ F

Time = ~ 60 sec ~125 sec ~188 sec ~240 sec

Fig. 9—Selected photographs of the test (see Fig. 8)

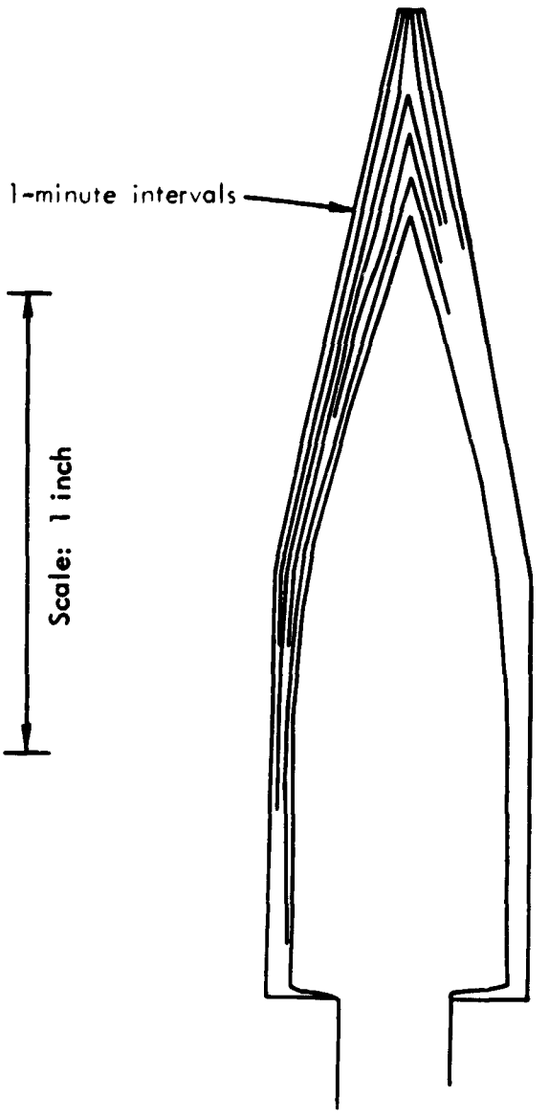

Fig. 10—Profiles of a 25-degree, flat-nosed cone with cylindrical afterbody at 1-minute intervals; $M = 3.05$, $P_0 = 735$ mm Hg, $T_0 = 138°$ F

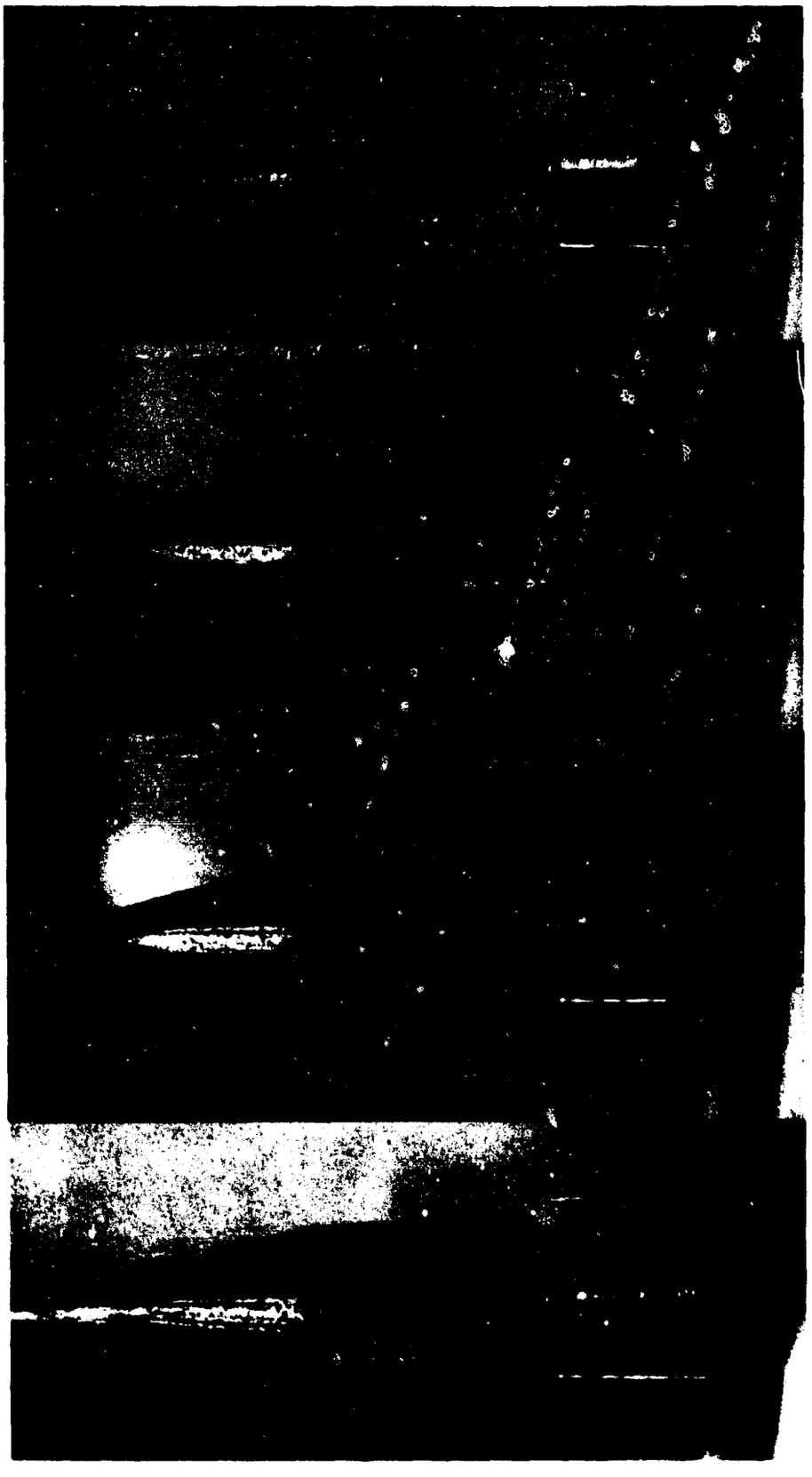

Fig. 11—Selected photographs of the test (see Fig. 10)

Figures 12 and 13 show test results from the same body at an angle of incidence. A spiral groove has developed at the tip, as in the case of the yawed 15-deg cone. In this model the deepening groove into which the tip gradually recesses produced a wedge-like nose after about 4 minutes (the leading edge is in the plane of the photographs). This led to an interestingly nonuniform and asymmetric sublimation of the afterbody, the shape of which after 6 minutes is sketched in Fig. 12.

ABLATION OF BODIES WITH REGIONS OF SEPARATED FLOW

Figures 14 and 15 show the erosion of a cross-stream notch. Figure 16 shows a similar cross-stream notch having a smaller initial length-to-depth ratio. Such grooves disappear very rapidly, beginning in the high-heat-transfer region of the recompression step. The floor of the cavity, where heat transfer is low, is hardly eroded until the entire notch is erased. The behavior of such transverse grooves is in sharp contrast to that of streamwise grooves, which do not erode away.

Figures 17 and 18 show the history of a conical forebody terminating in an upstream-facing step. A region of high mass transfer upstream of the step can be immediately identified inside the cavity (downstream of the point of separation of the boundary layer on the cone). The existence of this region is inconsistent with theoretical models in which it is assumed that the internal, recirculating cavity flow is nearly dead. The face of the step, and in particular the recompression corner, appear to erode remarkably slowly, which is surprising. Note also the spots of recondensed material not only at the base of the model (as noted on other models), but also on the surface of the cylindrical afterbody downstream of the step. This indicates that the boundary layer never truly "reattaches," or at least that it is very much thickened by the reattachment process.

The model of Fig. 18 shows the results of an interaction between a tip-generated groove propagating downstream and the cavity, leading to an asymmetrical distortion of the flow field (the termination point of the groove on the first two photographs indicates the point at which

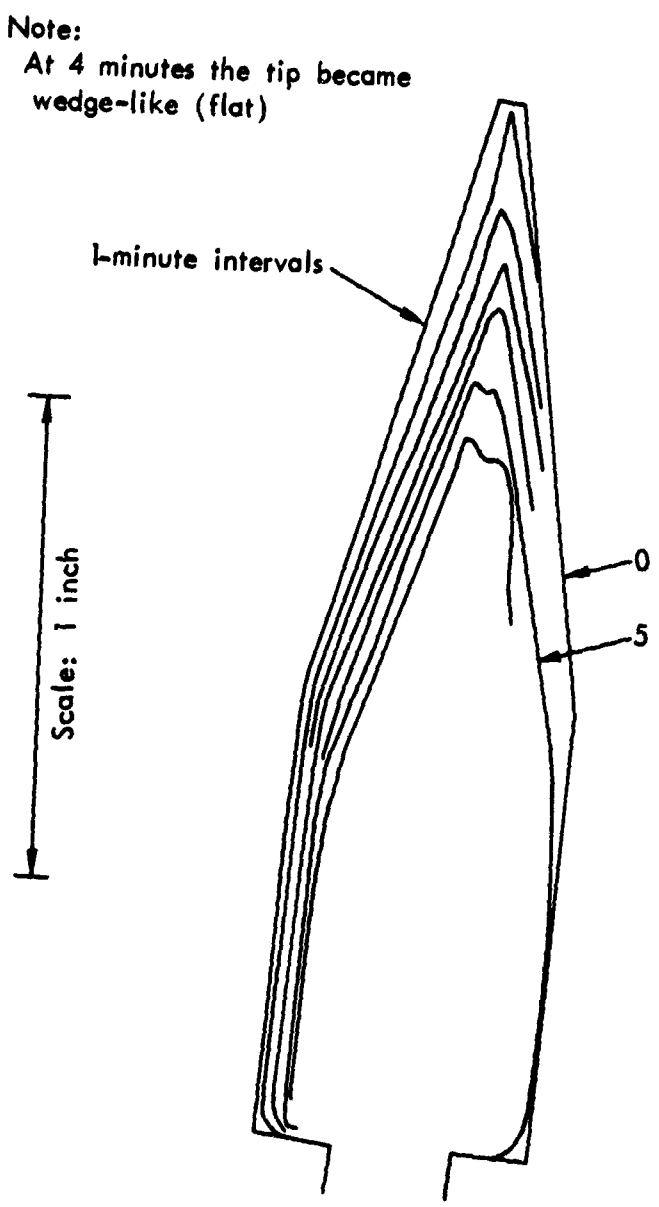

Fig. 12—Profiles of a 25-degree, flat-nosed cone-cylinder at 5 degrees incidence at 1-minute intervals; camphor, $M = 3\ 05$, $P_o = 735$ mm Hg, $T_o = 140°F$

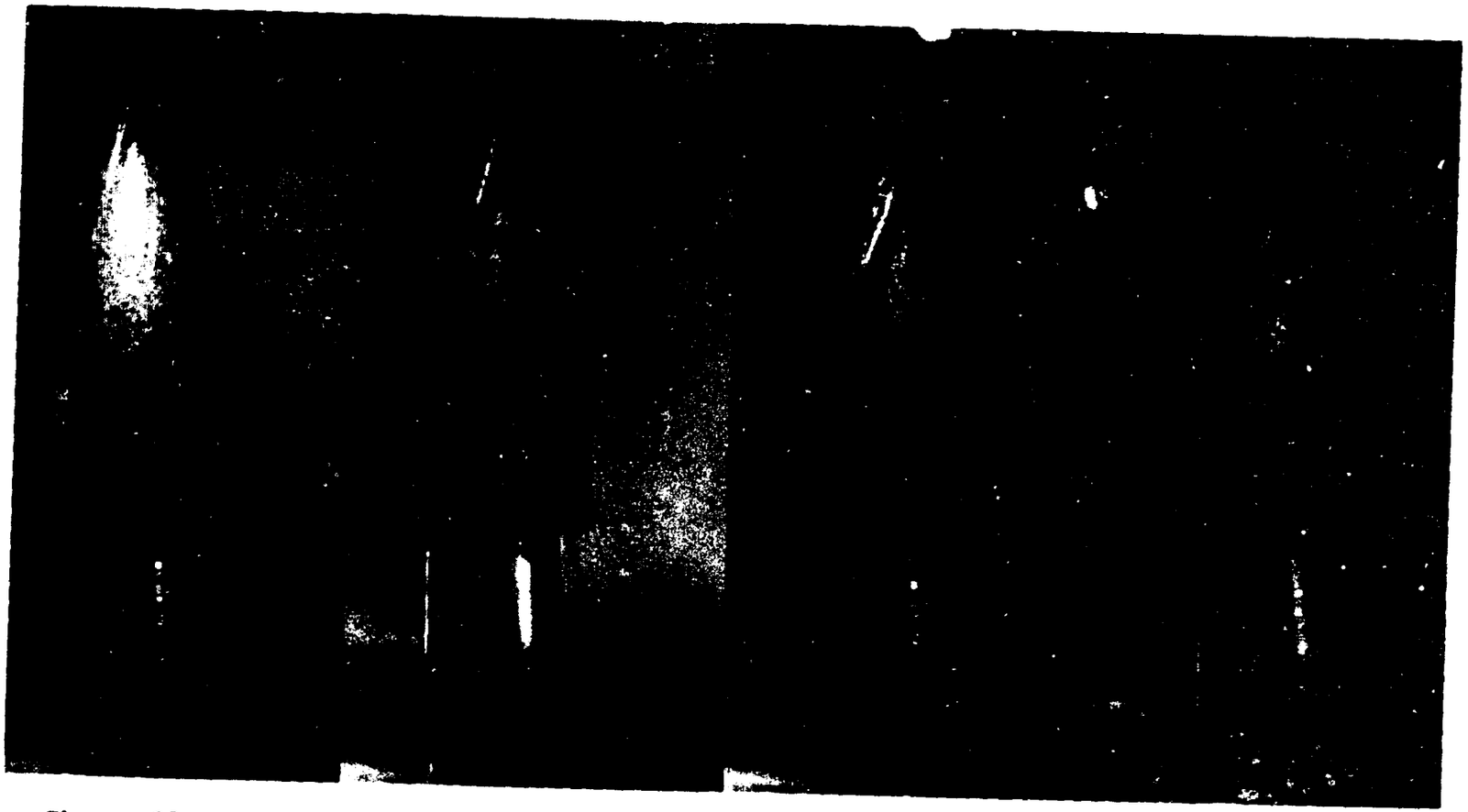

Time = 85 sec 140 sec 192 sec 250 sec

Fig. 13—Selected photographs of the test (see Fig. 12)

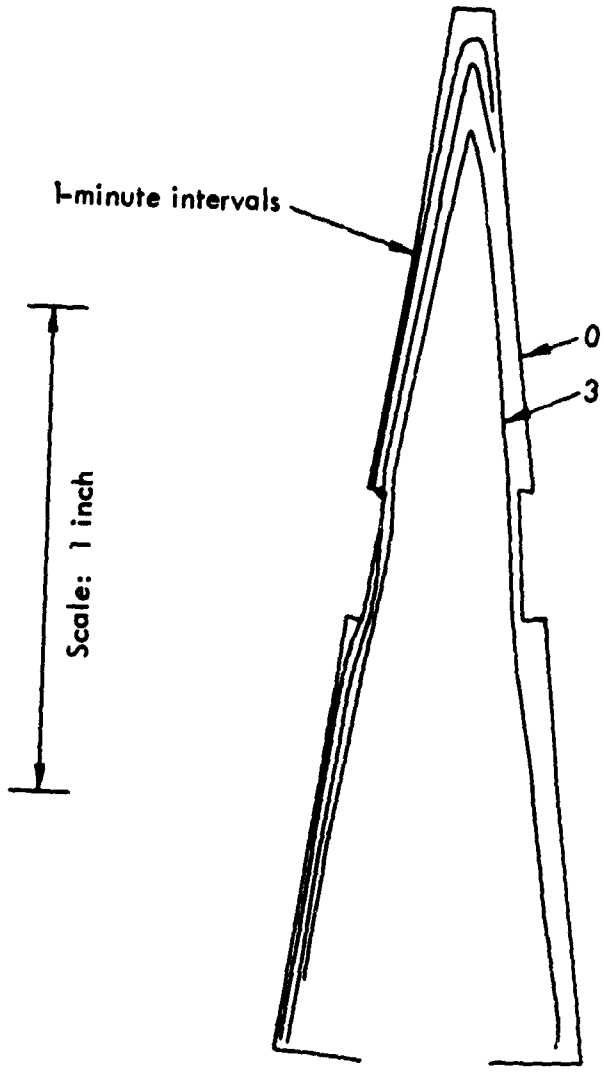

Fig. 14 — Profiles of a blunt-nosed, 15-degree cone with a rectangular transverse notch (0.050 in. deep, 0.250 in. long); camphor, $M = 3.05$, $P_0 = 735$ mm Hg, $T_0 = 146^\circ F$

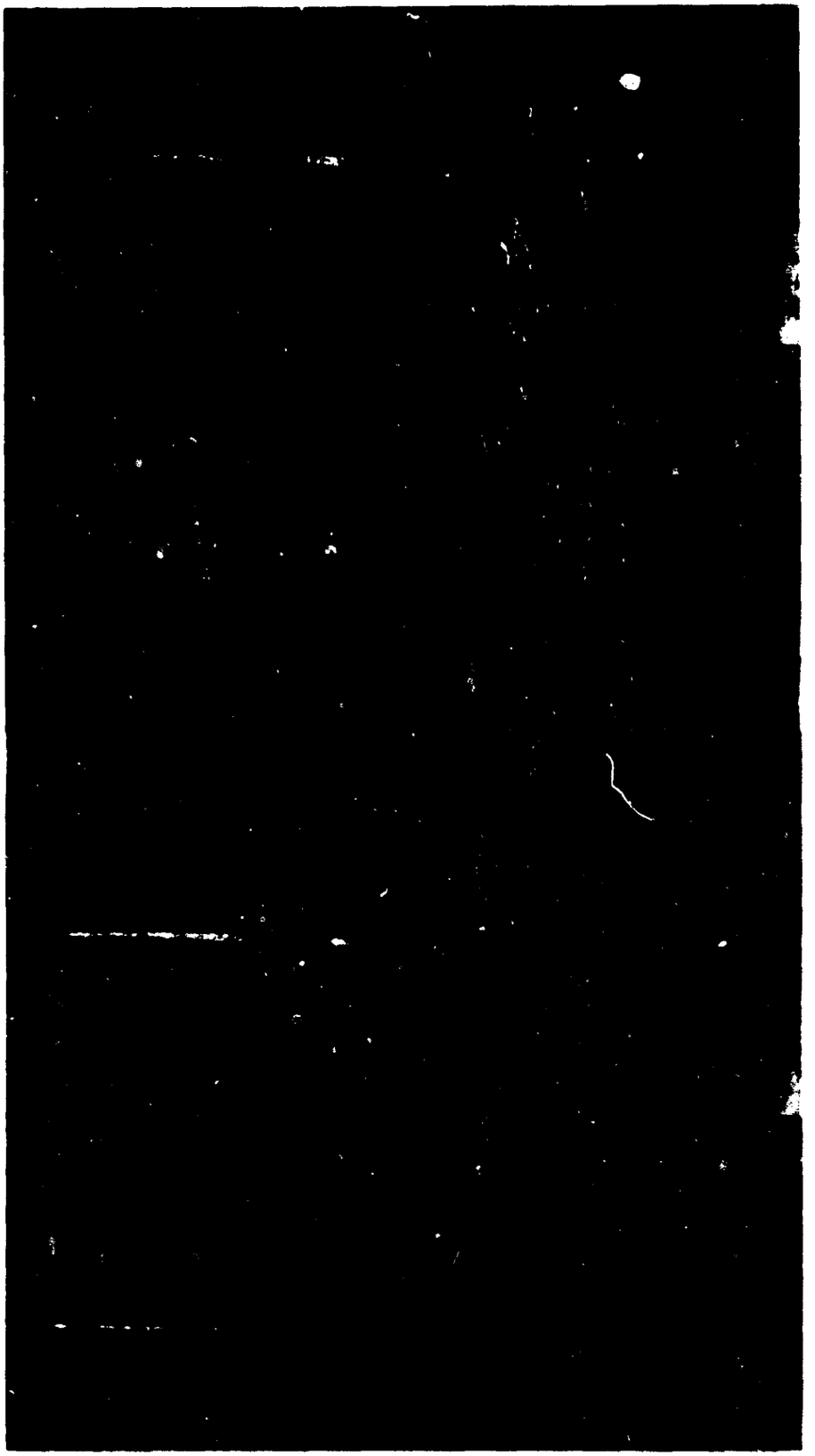

Fig. 15—Selected photographs of the test (see Fig. 14)

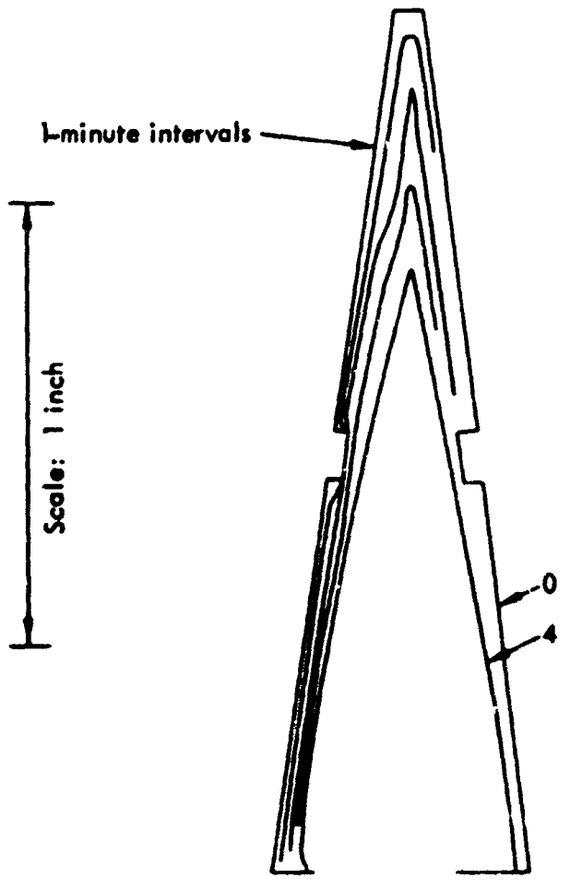

Fig. 16 — Profiles of a blunt-nosed, 15-degree cone with a rectangular transverse notch (0.050 in. deep, 0.100 in. long): camphor, M = 3.05, P_0 = 735 mm Hg, T_0 = 146° F

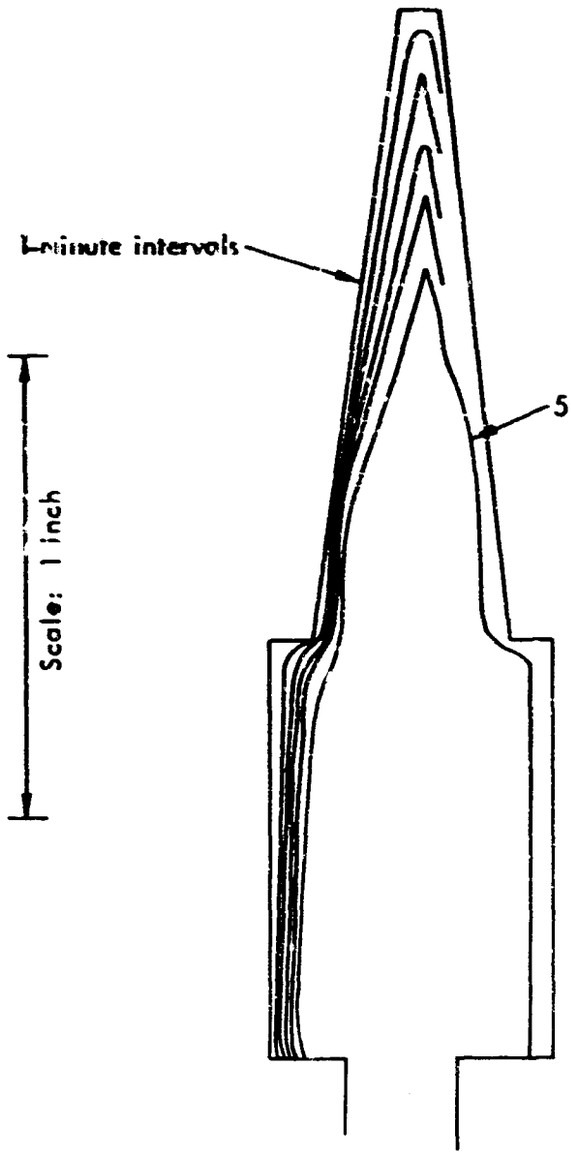

Fig. 17—Profiles of a flat-nosed, 15-degree cone with an upstream-facing step (0.0625 in. high); camphor, $M = 3.05$, $P_0 = 735$ mm Hg, $T_0 = 140°F$

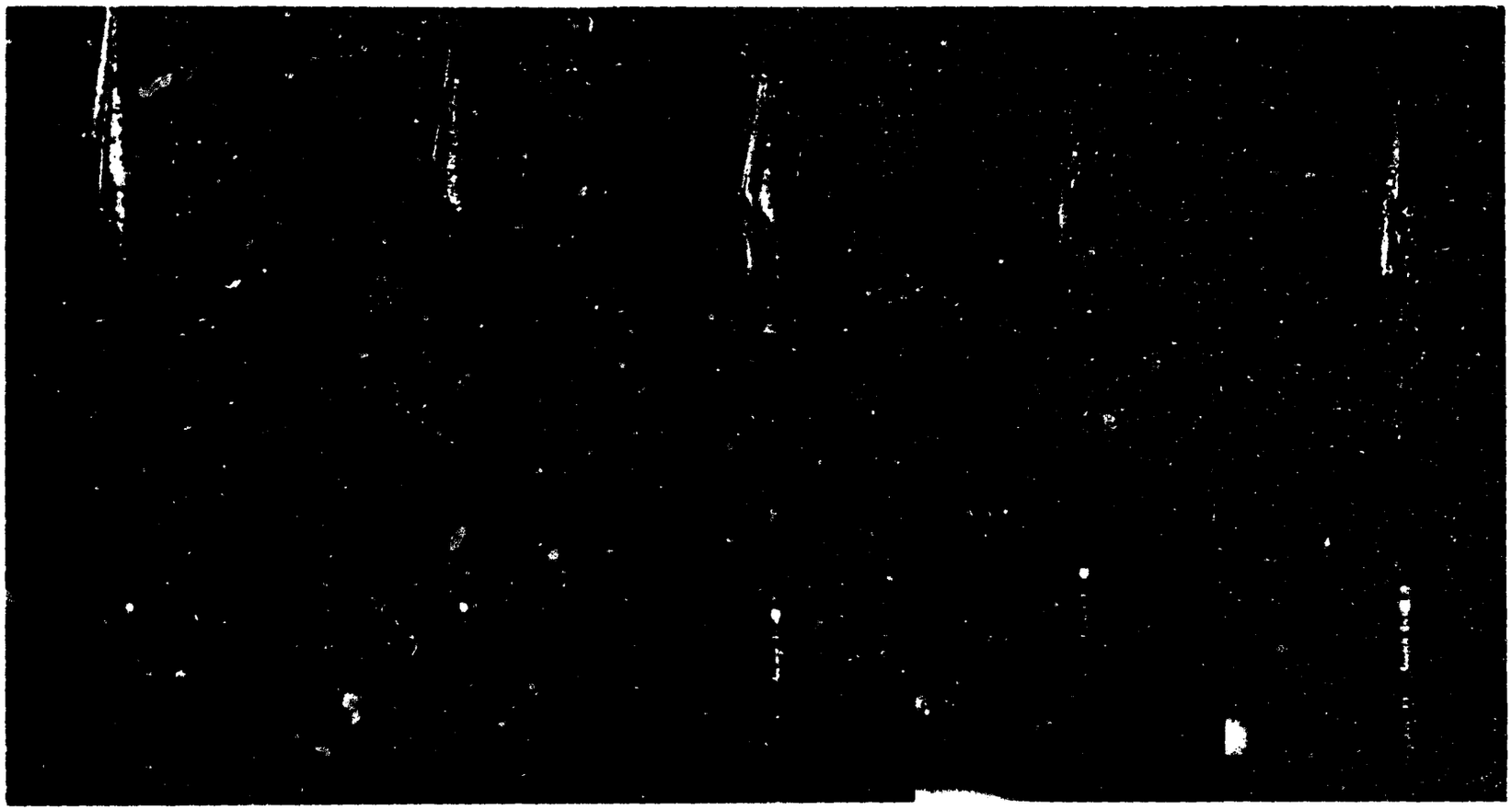

Time ~2 min ~3 min ~4 min ~5 min ~6 min

Fig. 18—Selected photographs of the test (see Fig. 17)

the boundary layer separates at the upstream tip of the cavity). Since upstream-facing cavities are known to be very unstable and sensitive to small nonuniformities, this observation is not surprising. The model is irregularly scarred with streamwise striations on the afterbody; however, these do not exhibit the homogeneity and uniformity of striations occurring when the basic profile is convex.

In contrast with the upstream-facing separation, the downstream-facing step, shown in Figs. 19 and 20, is eroded in a smooth and stable fashion. High heat transfer in the region of recompression causes the afterbody to become slightly convex (see first photograph) whereupon the regular pattern of streamwise grooves appears immediately. The grooves are spaced more widely here than in Fig. 11, a pattern associated with a boundary layer that is thicker after recompression than that on the cone forebody of Fig. 11. This observation is compatible with the suggested explanation that the forebody striations are due to a Görtler type of secondary flow structure.

Note that in the same period of time (and under the same free-stream conditions) the overall fineness ratio of the cone (Fig. 5) changed from .3 to .35, whereas that of the cone with a downstream-facing step (Figs. 19 and 20) changed from .3 to .285 [for the upstream-facing step (Figs. 17 and 18), the fineness ratio changed only slightly, from .28 to .295]. Associated with these changes is a significant change in the drag coefficient -- an increase in the case of the cone and a decrease in the case of the cone-step-cone model.

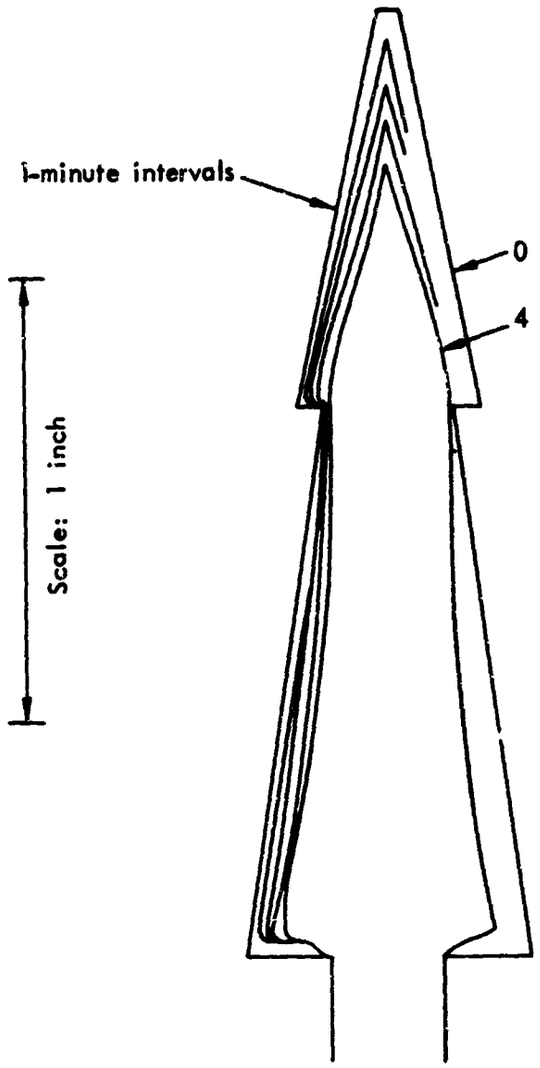

Fig. 19 — Profiles of 15-degree cones joined by a downstream-facing step; camphor, M = 3.05, P_0 = 735 mm Hg, T_0 = 141° F

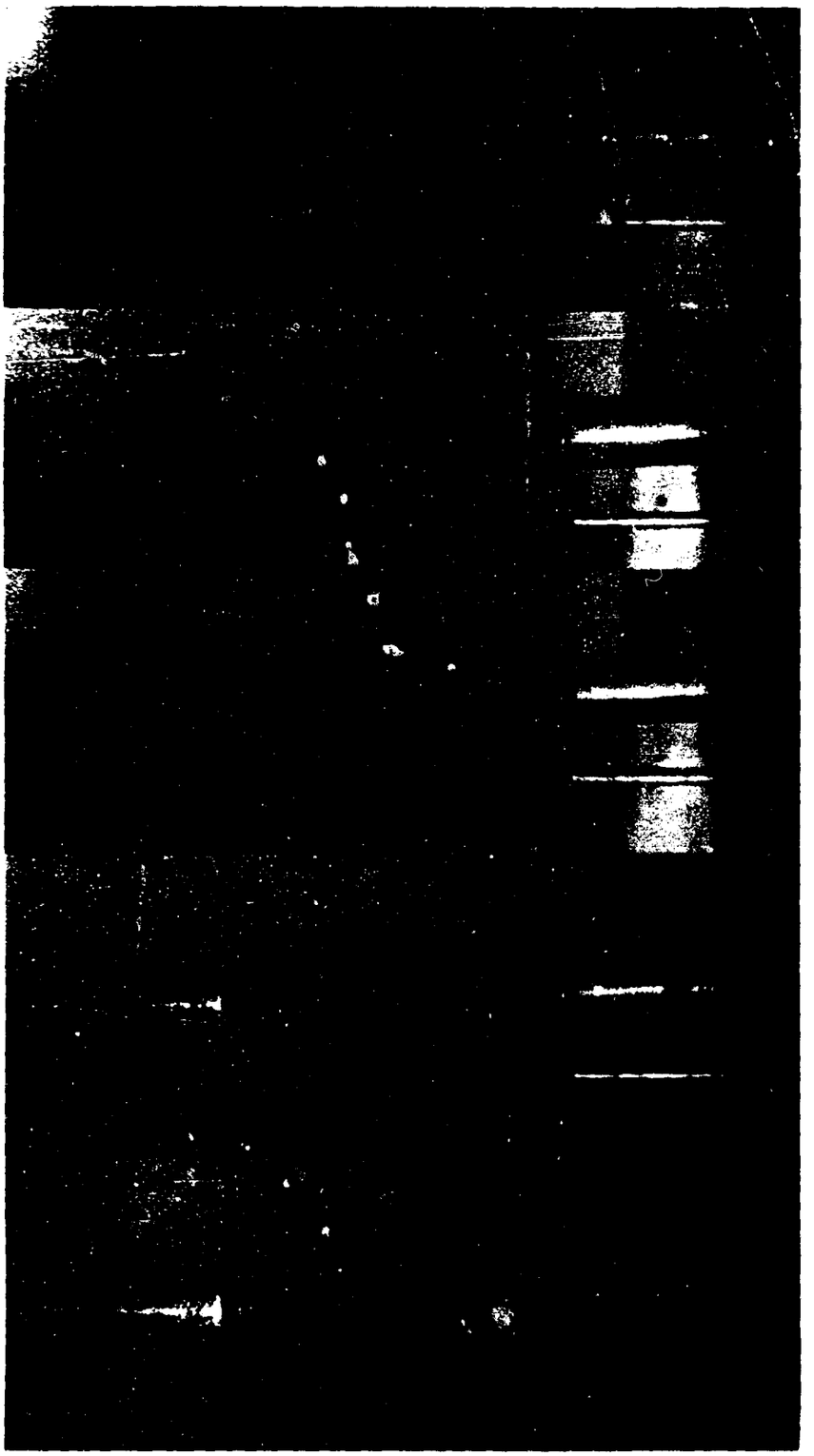

Fig. 20—Photographs of test (see Fig. 19)

V. DISCUSSION

In observing the sublimation of models in the tunnel, one can at all times follow and qualitatively interpret the history of their recession. The development of nonuniformities and streamwise scars can be observed and related to identifiable causes, such as, say, the way in which the needle tip erodes and shears off. The vacuum-sintered material used behaves very satisfactorily, even when sharp corners and steps are machined in it.

However, the observed profile of the model at any instant, which depends on the time integral of its previous history, exhibits variations which cannot be foreseen a priori. The most notable nonuniformities occur when the tip of the model recedes into the streamwise scars (grooves) that originated from the tip at any earlier time.

One of the most striking anomalies was recorded during tests with one 15-deg flat-nosed cone (Fig. 4) and with the flat-nosed 25-deg cone-cylinder (Fig. 10). Immediately after the start of the test and for a period of about 15 sec, camphor powder accumulated on the face of the model, causing an apparent increase of 0.2 inches in the total length of the 15-deg cone! (The 25-deg model evidenced less accumulation, and the material was not uniformly distributed over the face of the nose.) The material accumulated has the appearance of a fairly loose and porous powder; we noticed it during the test but did not realize that it was actually deposited upstream of the initial station of the nose until the film with its reference markings was developed. The observation is accurate, but cannot be explained at this time. In any case, about 30 to 45 sec after start, the deposit disappeared and the shoulder gradually eroded to a rounded shape and finally to a sharp point.

In general, a blunt-nosed cone initially becomes slightly concave downstream of the nose/afterbody junction, apparently as the result of the total or near-separation of the boundary layer at the corner and

its subsequent re-establishment on the afterbody.* The subsequent detailed evolution of the profile is intimately related to the history of the tip: In Figs. 3 and 4 the shoulder erodes, forms a sharp tip which recedes, and then "catches up" with the concave surface rather rapidly, forming a biconvex, ogival final shape. In Fig. 11, on the other hand, the erosion of the shoulder leaves a needle tip of remarkable length (see the photograph taken at 125 sec) and a distinctly convex forebody profile. Ultimately, this body also "relaxes" to the more stable ogival shape like the others.

With camphor, the tip always tends to form a needle point under the present test conditions. Typically, the needle has a .01-inch diameter at the base and a .10-inch length (see, for example, Fig. 5). The needle erodes by crumbling more or less randomly, and an observer often has the impression of seeing the body escape upstream into the needle. How the needle behaves is critically important; it is stronger (and longer) on cones with a larger divergence angle. The formation of the needle may be an "over-shoot" associated with the erosion of a blunt-nosed cone, and may fail to take place on bodies which are initially sharp. One would also expect there to be, for each specific ablator, a critical divergence angle beyond which the phenomenon would not occur; naphthalene, for example, did not behave in this way.

On a slightly coarser scale, the sublimation of these simple and composite cones is quite reproducible. The general features of the evolution of the shape were presented in the preceding section. A characteristic velocity of the overall process can be identified as the streamwise recession rate of the tip, at least during the period after it becomes pointed. Figure 21 shows tip-recession rates for camphor cones at low stagnation temperatures, and Fig. 22 gives similar data for higher temperatures. After an initial period of adjustment the recession of the tip becomes remarkably linear. There is some scatter in the results, possibly due to (a) insufficiently close

---

*This type of behavior has been observed before and interpreted in terms of laminar/turbulent transition. Although transition does not seem to be the cause here, it would have a similar effect.

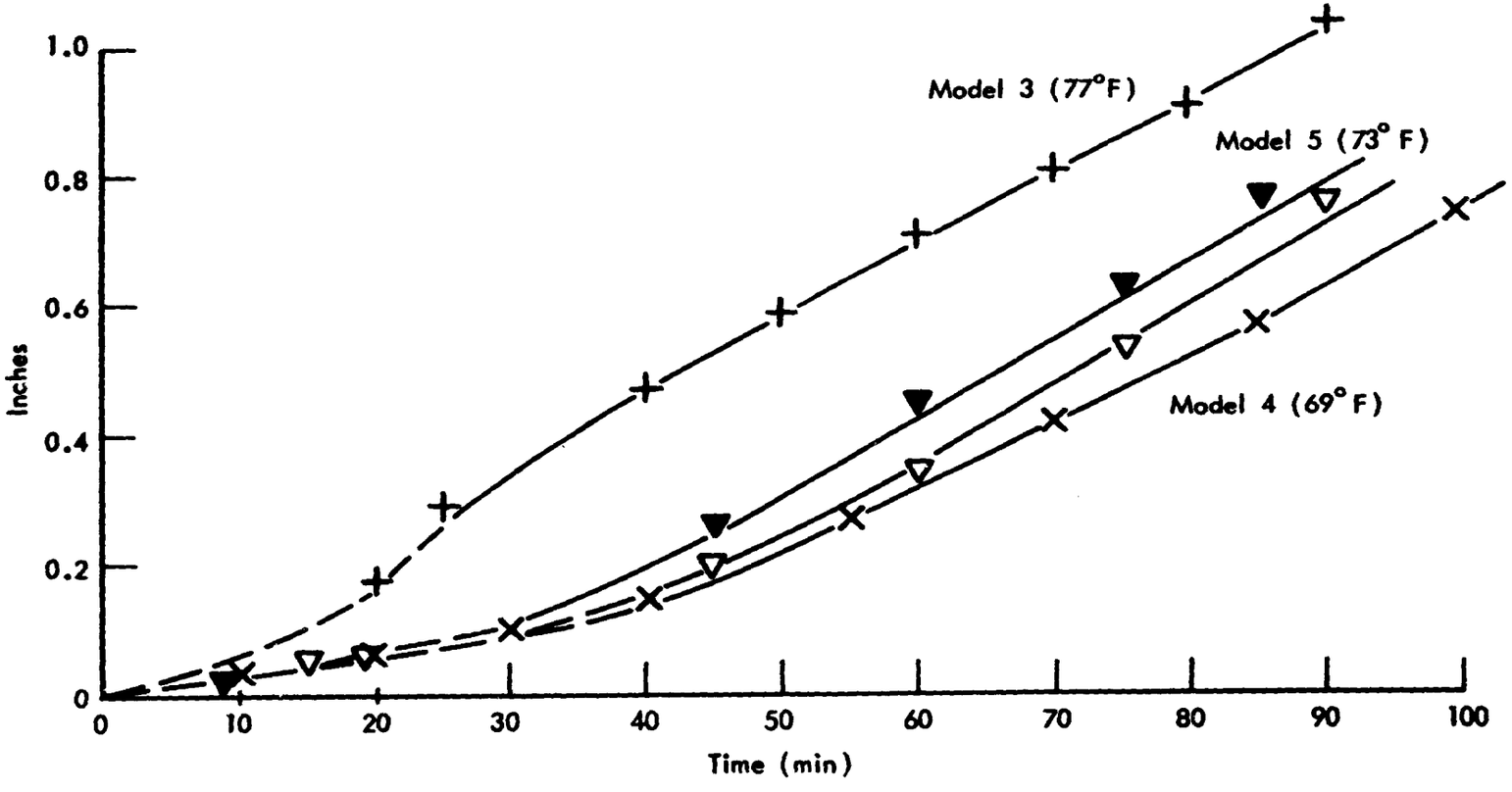

Fig. 21—Tip recession rate of flat-faced cones; camphor, P_0 = 1 atm, T_0 = approx 70° F

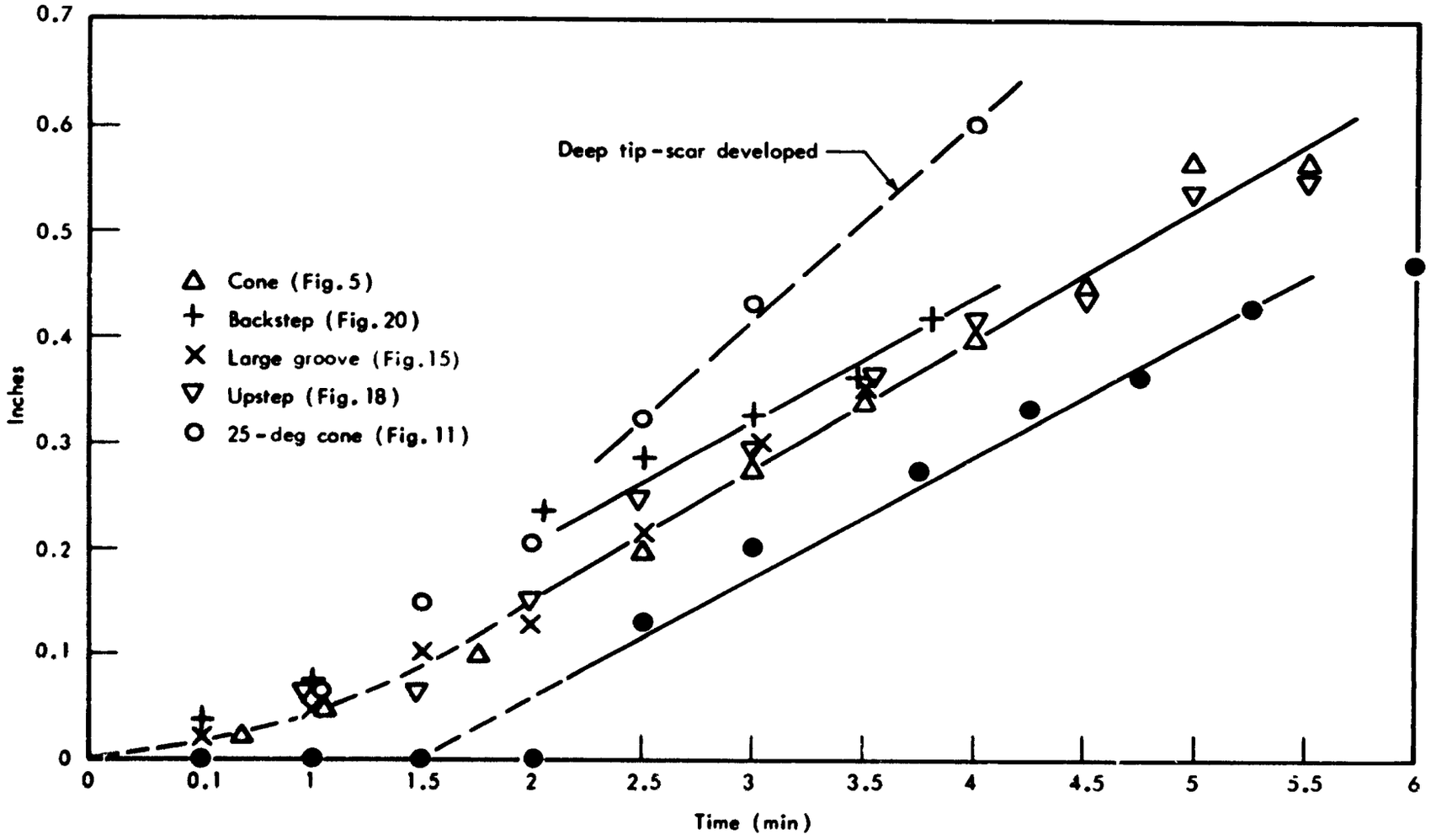

Fig. 22 - Tip recession rate of flat-nosed cones and other conical bodies; camphor, P_0 = 1 atm, T_0 = approx 140°F

control over the stagnation temperature, which varied in some of the tests by 10°, and (b) the persistence of the influence of the initial period and the effect of streamwise scars formed in that time. It is notable that the high recession rates in Fig. 22 occurred with a model on which a deep groove formed at the tip very early.

Neither the divergence angle of the conical afterbody nor the incidence of the model to the flow seems to affect the recession rate.

The constancy of the tip-recession velocity and its independence of the geometry of the body suggest immediately the influence of a thermochemical-limit phenomemon which is independent of the local transfer properties of the boundary layer. Such a phenomenon was considered in Ref. 9, where it was shown that downstream of a sharp tip (the origin of the boundary layer) there is a zone characterized by a length δ which is defined by physical constants of the subliming material and free-stream parameters only, and within which the sublimation process is controlled by the kinetics of phase change and not by the boundary-layer diffusion mechanism. The blowing parameter tends to zero at the tip, the surface temperature tends to the adiabatic recovery temperature of the free stream, and the mass-transfer rate tends to a maximum which is proportional to

$$\dot{m} \sim \frac{n_s}{\sqrt{T_{aw}}} [P_s]_{T_{aw}}$$

where P_s is the equilibrium phase-change pressure of the pure sublimators taken at the adiabatic recovery temperature of the free stream and n_s is the molecular weight of the sublimator.

Using data for camphor, one obtains the following values:

Parameter	Test Series I	Test Series II
(a) Stagnation temperature:	70°F	140°F
(b) Scaling parameter, $n_s P_s / \sqrt{T_s}$ $\left[\frac{\text{mm Hg}}{(^{\circ}\text{R})^{1/2}}\right]$:	.117	1.20

(c)	Mean tip recession rate, inches/min:	.0118	.125
(d)	$\frac{\text{Scaling parameter (b)}}{\text{Tip recession rate (c)}}$:	9.9	9.6

The general accord of these exploratory experimental trends with predictions of the theory suggests that further study may prove to be fruitful.

Figure 23 shows tip recession rates for the three naphthalene models tested. Although trends in these data are the same as for the camphor model, one cannot expect a quantitative comparison with the theory, which applies only to pointed bodies, and the naphthalene models never formed a sharp tip. Moreover, there was a considerable difference in the initial bluntness of the models tested at the two stagnation temperatures.

A few observations regarding the occurrence and behavior of grooves and surface scars are described below.

We did not observe the cross-hatching pattern mentioned in the Introduction. This accords with the experience of other investigators.[14] This pattern has not been noticed except in regions of transition or turbulence.

Towards the end of the tests, we did observe on some models irregular, streamwise striations, together with cross-stream (irregular) "wavelets,"[1] on the downstream third of the model's surface. However, this occurred only after the model had ablated quite a distance, exposing the material around the base of the stub of the sting imbedded in the camphor. This stub is screwed into the piston during the compression process, and the powder often did not sinter around it as well as it did in the bulk of the material. Thus the surface markings may well be due to the different properties of this portion of the model (e.g., lower shear strength or inhomogeneous structure).

The deep streamwise grooves, referred to as "scars" in the preceding discussion, most often originated at the very tip, and formed all along the length of the model at once. This indicates that, rather than being "eaten out" of the downstream edge of the disturbance, the

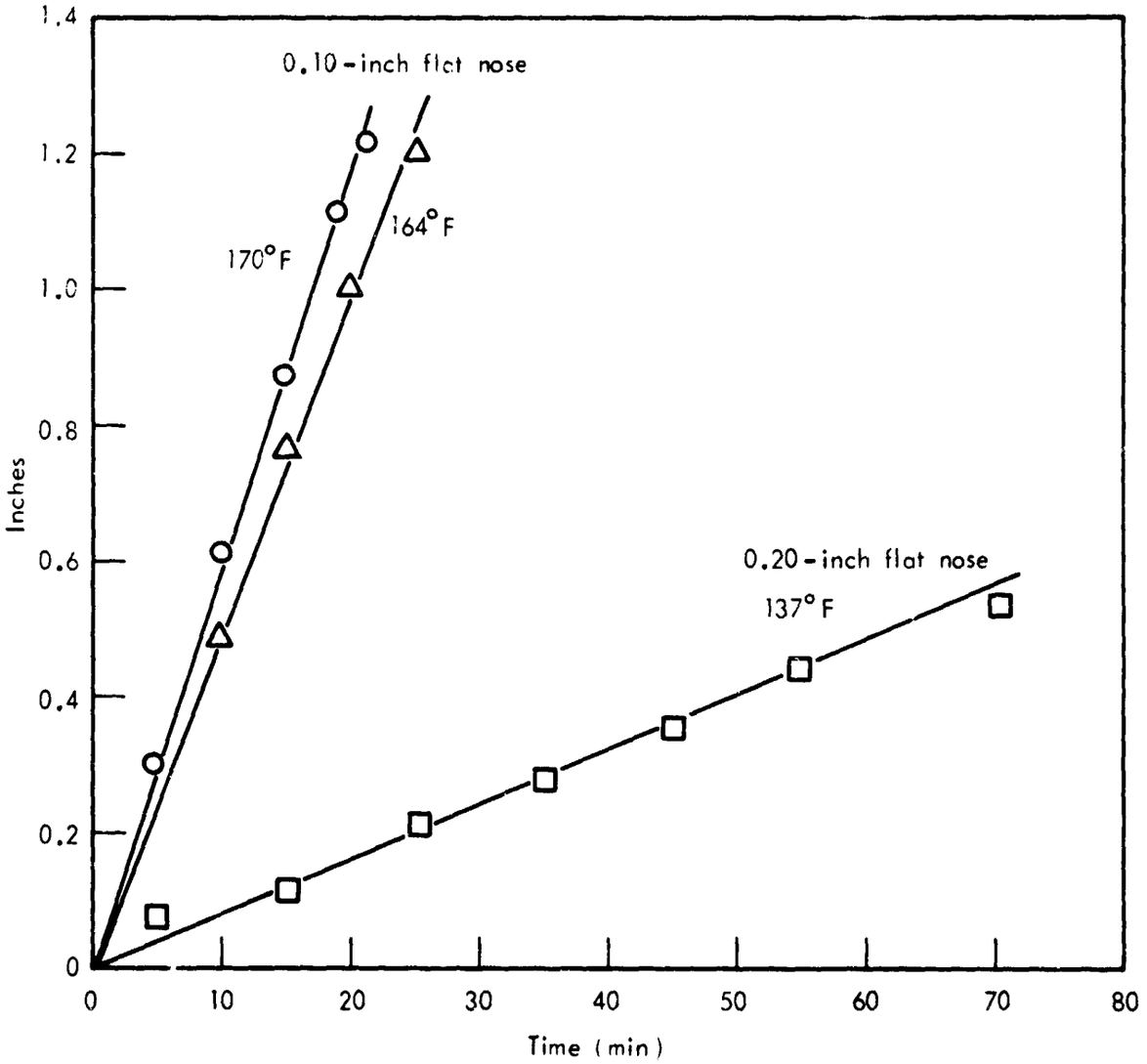

Fig. 23—Tip recession rate of three flat-faced naphthalene cones

grooves result from a disturbance in the boundary layer, such as a vortex with its axis parallel to the flow, which is attached at the disturbance and convected downstream with a velocity of the order of the free-stream velocity.

There appears to be a minimum depth of a streamwise groove below which it is unstable and disappears when the disturbance causing it is removed, and above which it persists, apparently sustaining the disturbance in the boundary layer. One can observe many weak striations that appear at the tip as it erodes and disappear if the tip changes shape (the typical time associated with this process is estimated to be 15 sec for the camphor models at 140°F). If the disturbance persists long enough to scar the surface critically, the groove remains.

An example of this process is seen in Fig. 11. The pattern of striations visible on the forebody was associated in the foregoing discussion with a Görtler instability of the flow over a concave surface. The grooves are not deep, and as the surface becomes convex (~ 220 sec) are totally erased.

The sensitivity of this phenomenon to vortical disturbances in the boundary layer is remarkable. A subliming surface may indeed one day be used to detect such phenomena, which would otherwise be virtually unmeasurable.

Finally, the erosion of the notched models indicates that transverse grooves or cracks are "unstable" in the sense that they cause a disturbance which erases them, contrary to "stable" streamwise grooves.

VI. CONCLUSIONS

The method of sintering a deaerated powder described herein proved to provide a far stronger and more homogeneous block of camphor or naphthalene, from which one can machine wind-tunnel models for the study of sublimation in high-speed flow.

A series of models fabricated by this method, comprising blunt-nosed cones and composite models with downstream- and upstream-facing steps, notches, and corners, was subjected to an exploratory study. The erosion of these shapes follows a logical pattern, reproducible in its gross features but subject to local, random variations associated with the history of the erosion of the tip. It seems feasible and useful to consider further the use of certain of these features (for instance, downstream-facing steps) in connection with prescribing a drag-ablation profile for a reentry trajectory.

It was demonstrated that there are consistently reproducible conditions in which the blunt nose of a body becomes pointed in the absence of laminar/turbulent transition and tends to form a sharp needle. The recession of a pointed tip appears to be linear with time, and tentatively verifies the predictions derived from a theory exploring the kinetic-rate-limited sublimation. Further study is indicated to achieve a thorough understanding of these phenomena.

It was shown that cross-stream grooves tend to be erased, whereas streamwise grooves couple with the boundary layer in such a way as to be perpetuated. There seems to be a critical depth at which such grooves persist; this is also a promising subject for further quantitative study using the present experimental technique.

A regular pattern of striations was consistently observed on concave surfaces. It is suggested that this is evidence of a Görtler instability. Such vortex patterns "freeze" into a homogeneous subliming surface remarkably clearly, so that such a surface may well prove to be a more sensitive index of their occurrence than any other instrument.

Appendix A*

AEROTHERMODYNAMICS OF AIR/CAMPHOR AND AIR/NAPHTHALENE SYSTEMS

The convective-transfer characteristics of a boundary layer with wall blowing are given by the well-known linear approximation

$$\frac{C_H}{C_{H_0}} = 1 - KB \qquad \text{(A-1)}$$

where B is the blowing parameter defined by

$$B = \frac{\dot{m}}{\rho_e u_e C_{H_0}} \qquad \text{(A-2)}$$

and C_H and C_{H_0} are the Stanton numbers with and without blowing (under identical free-stream conditions), respectively.

The present calculations are based on the following correlation applicable to laminar flow:[11]

$$\frac{C_H}{C_{H_0}} = 1 - 1.82\left[\left(\frac{\rho_2}{\rho_s}\right)^{1/3} BC_{H_0}\sqrt{Re_x}\right] \qquad \text{(A-3)}$$

where the no-blowing heat-transfer characteristic of the compressible boundary layer, represented by the product $(C_{H_0}\sqrt{Re_x})$, is derived from van Driest's[12] calculations.

We now introduce a second blowing parameter,[13] commonly denoted by B':

---

*This section is based on the work of Sayano.[8] A more complete discussion of the various parameters is to be found in that source.

$$B' = \frac{\dot{m}}{\rho_e u_e C_H} = B \frac{C_{H_0}}{C_H} \tag{A-4}$$

If heat losses by radiation and by transient conduction into the body are neglected, so that all the heat transferred to the surface is ultimately absorbed by phase change, a heat and mass balance on an element of surface (for Prandtl and Lewis numbers of unity) provides the relation

$$B' = \frac{h_{2e} - h_{2w} + u_e^2/2}{L_E + L_T} \tag{A-5}$$

where L_E and L_T are the heat of sublimation and the heat capacity of the solid from some initial temperature T_i to the temperature of phase change (the wall temperature). For a given set of free-stream conditions and properties of the substance, Eq. (A-5) is a function of wall temperature only.

The concentration of the sublimate at the surface, and thus its partial pressure, is obtained from integration of the mass diffusion equation, and is expressed in terms of B' as

$$\frac{\rho_s}{\rho} = \frac{B'}{B' + 1} \tag{A-6}$$

If the vapor is assumed to behave as a perfect gas,

$$B' = \left(\frac{\mathcal{M}_s}{\mathcal{M}_2}\right)\left(\frac{P_s/P}{1 - P_s/P}\right) \tag{A-7}$$

The saturation pressure P_s is uniquely determined by the wall temperature by use of the phase diagram of the substance. Consequently Eqs. (A-6) and (A-7) uniquely determine B' as a function of the free-stream parameters.

Parametric maps of surface static pressure and tunnel stagnation temperature are shown in Figs. A-1 and A-2 for camphor and naphthalene, respectively.

Figures A-3 and A-4 show cross plots of C_H/C_{H_0} versus B, including values of B', calculated by use of the blockage equation (A-3). The variation of $C_{H_0}\sqrt{Re_x}$ with Mach number and wall-to-free-stream temperature is shown in detail in Fig. A-5.[11] With the aid of this figure, the actual rate of surface recession at a station one inch downstream of the leading edge in a flow without pressure gradients was calculated, as shown in Figs. A-6 and A-7 for camphor and naphthalene, respectively.

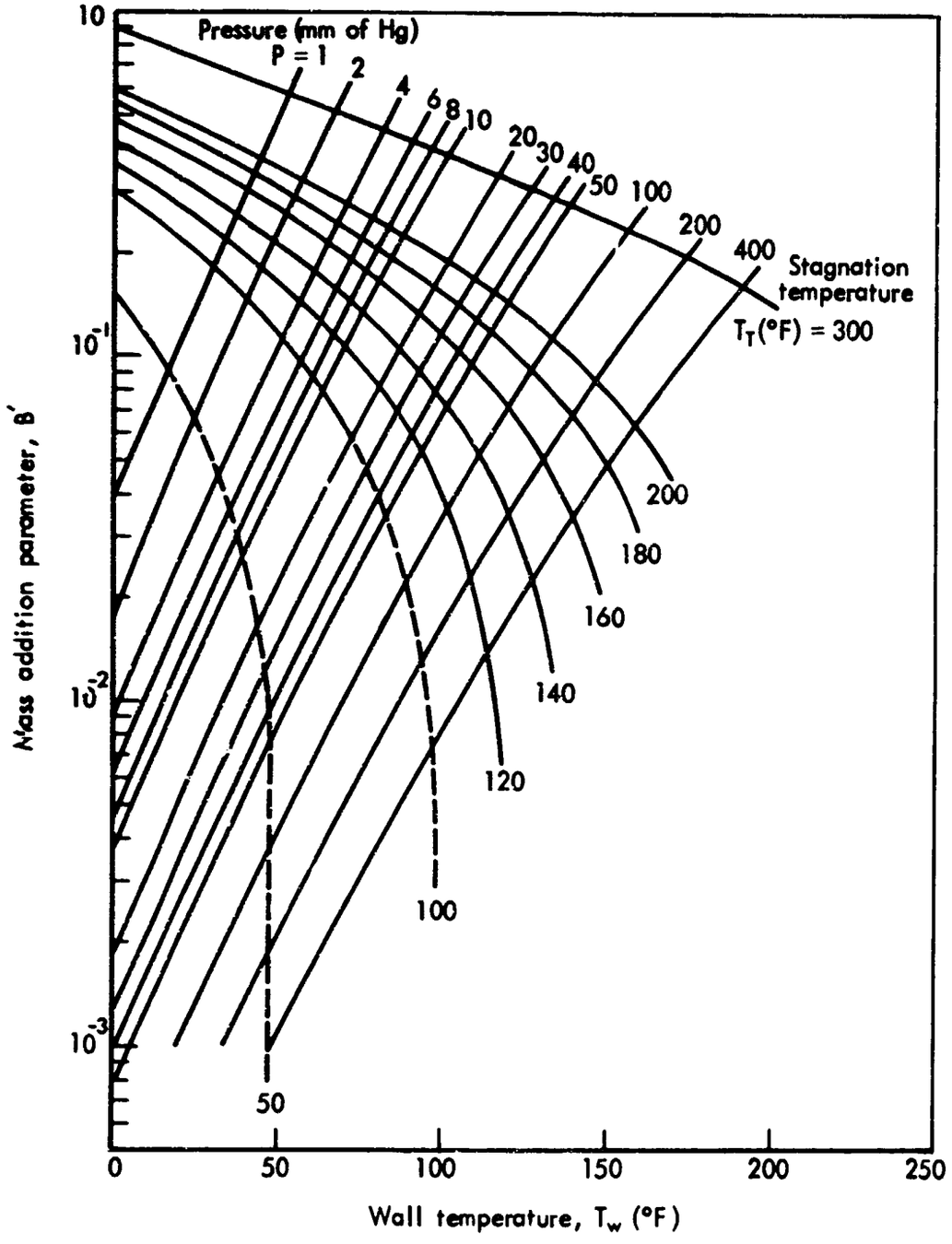

Fig. A-1—Variation of mass addition parameter with wall temperature and static pressure for various total temperatures; camphor/air system, σ = Sc = Le = 1.0

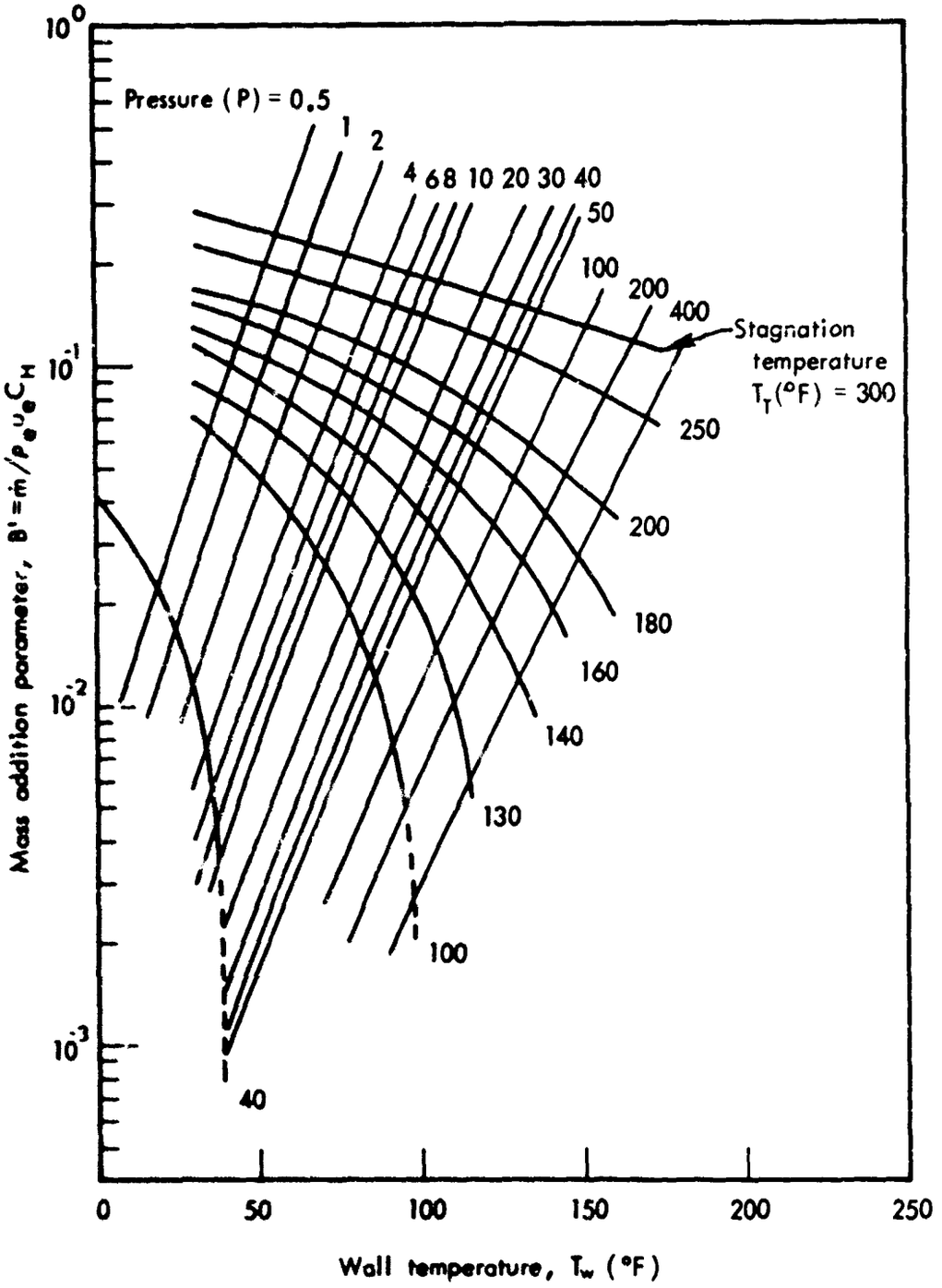

Fig. A-2—Variation of mass addition parameter with wall temperature and static pressure for given total temperature; naphthalene/air system, σ = 1.0, Sc = Le = 1.0

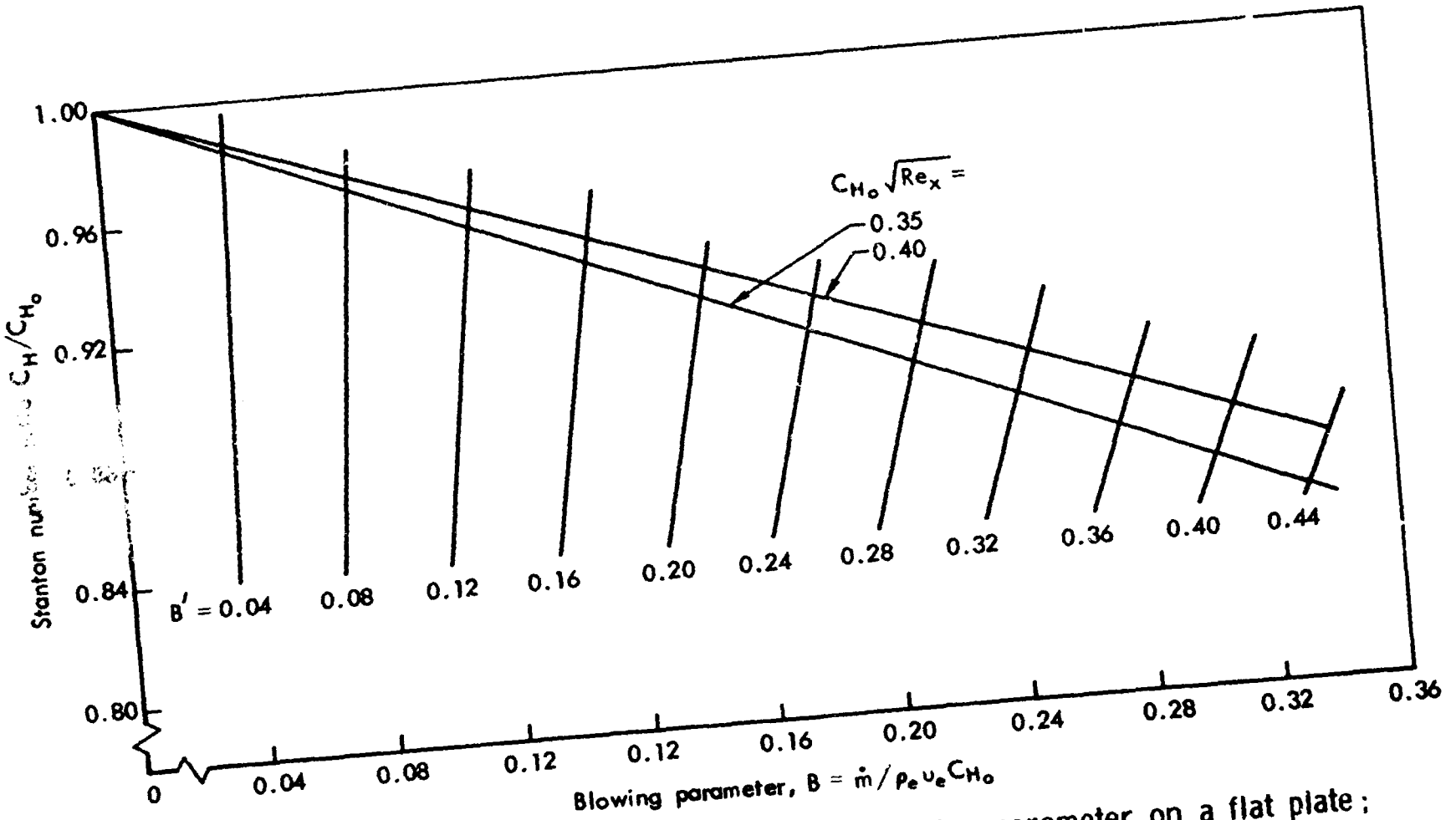

Fig. A-3—Variation of Stanton number with blowing parameter on a flat plate; camphor/air system, laminar flow

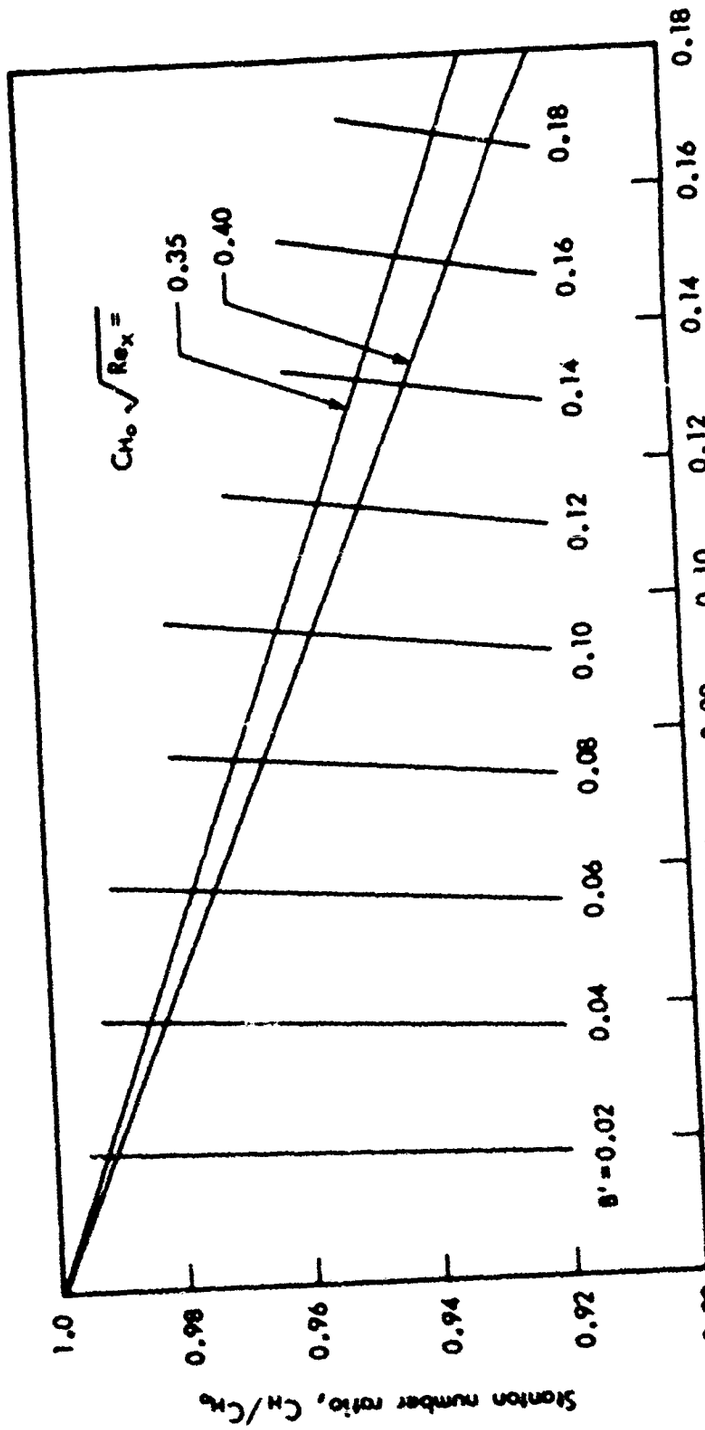

Fig. A-4—Variation of Stanton number with blowing parameter on a flat plate; naphthalene/air system, laminar flow

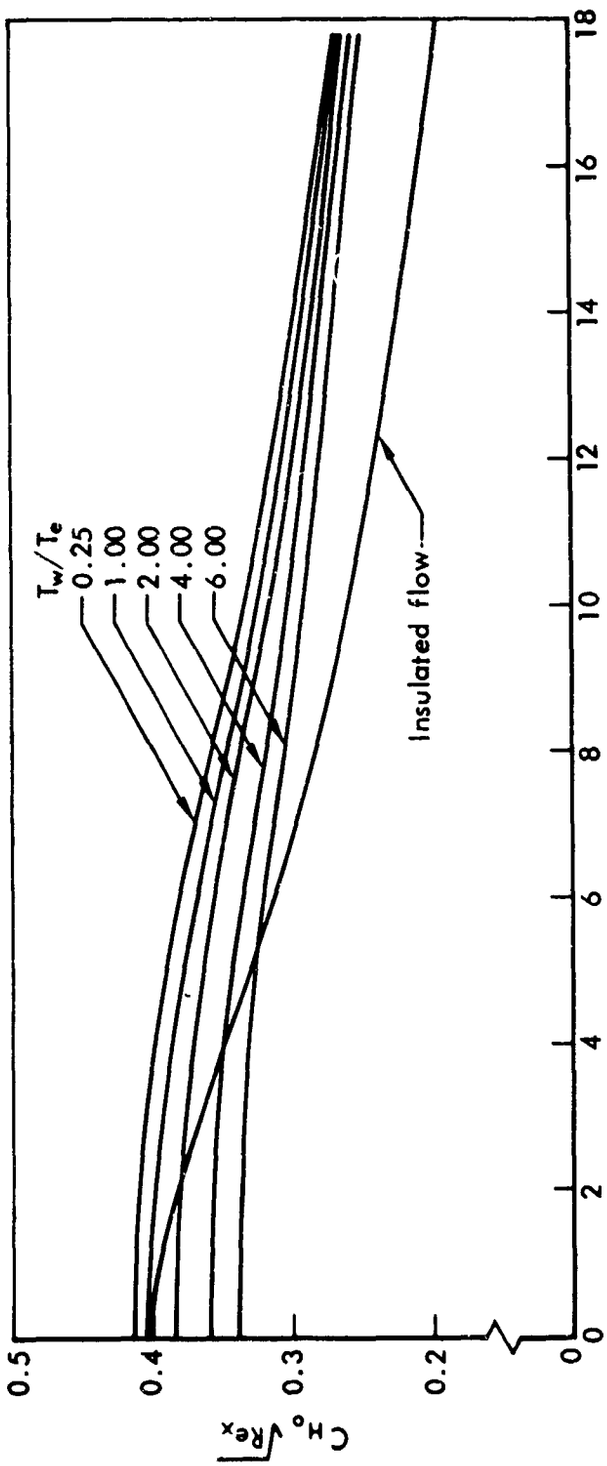

Fig. A-5—Local heat-transfer coefficient for laminar compressible boundary layer; flat plate, $\sigma = 0.75$ (Van Driest theory)

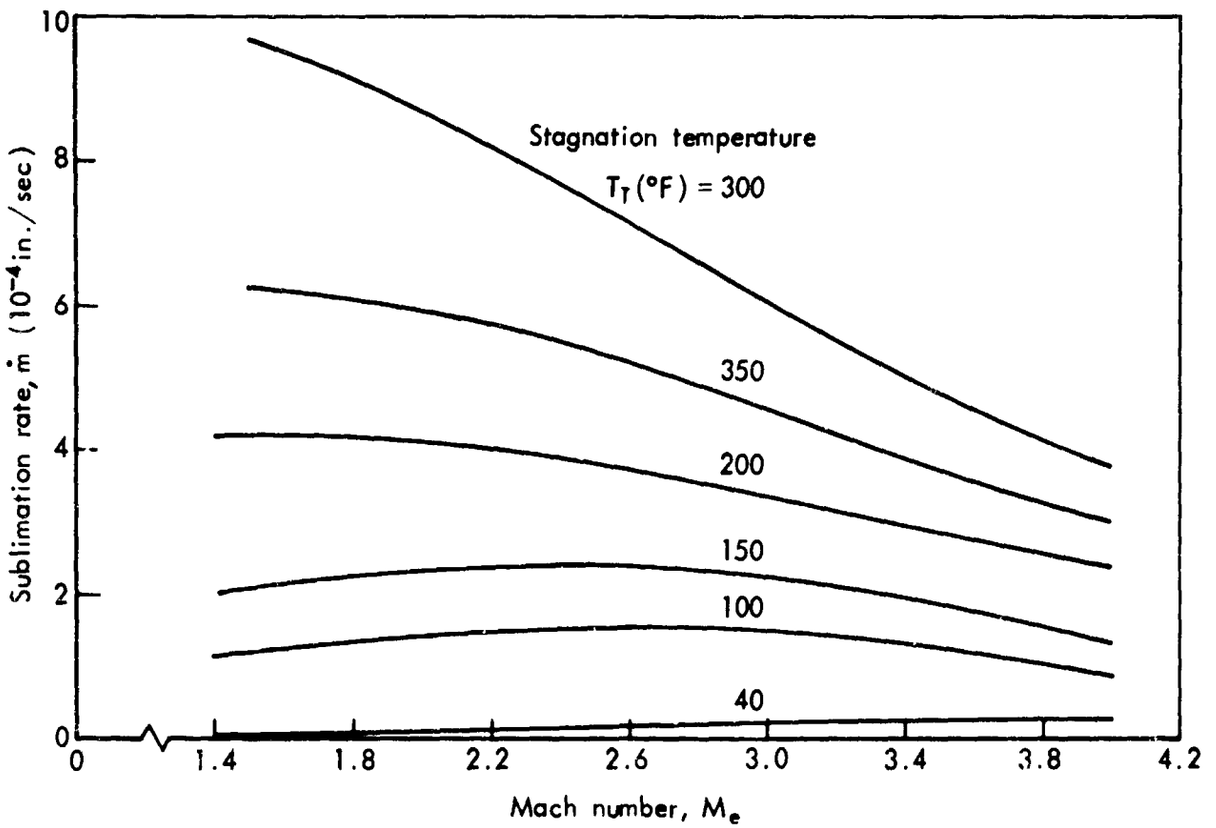

Fig. A-6—Surface recession rate in uniform flow at x = 1 inch; camphor/air system, σ = Sc = Le = 1.0, stagnation pressure of 1 atm

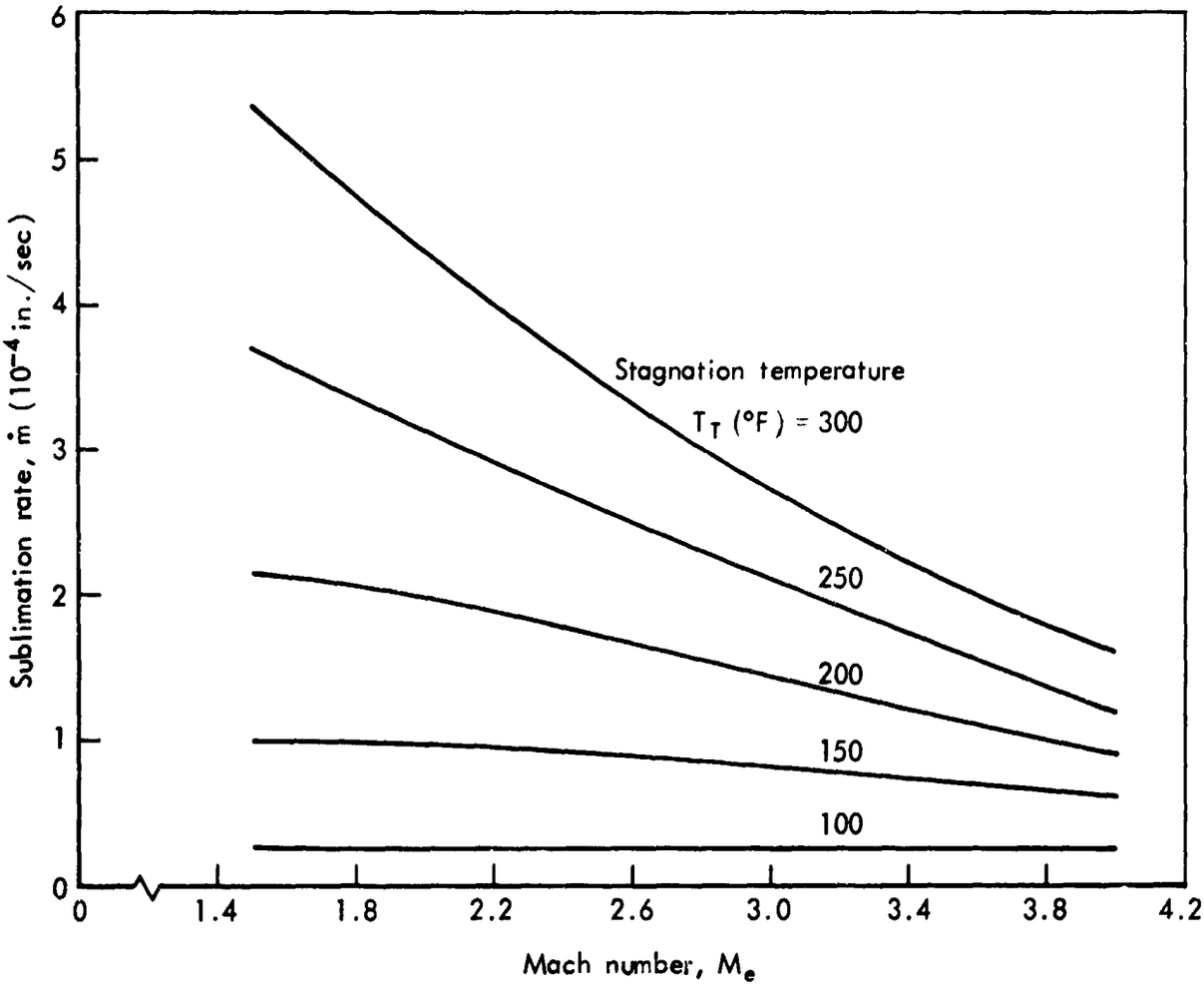

Fig. A-7—Surface recession for uniform free stream at x = 1 inch; naphthalene/air system, σ = Le = Sc = 1.0 stagnation pressure of 1 atm

Appendix B

TECHNIQUES OF CASTING AND SINTERING THE MODELS

A. RECRYSTALLIZED MODELS: CASTING AND TESTING

Direct recrystallization in a mold under a variety of cooling schedules and pressures results in the growth of relatively large crystals. These can be more or less disoriented by proper design of the boundary of the mold (the heat sink), where crystallization begins. In the present experiments attempts were made to cast cylinders with and without central stems in molds made of both metal and low-thermal-conductivity plastics. The walls of the molds used were either smooth, resulting in the growth of long, radially distributed crystals, or wavy, resulting in a disoriented crystal growth. However, in all cases the models were clearly crystalline.

All recrystallized models were subjected to two observational tests:

a. Static Sublimation. Cylinders 1/2 inch in diameter and 2 inches long were placed in an oven maintained at atmospheric pressure at 150°F. The behavior of the model as it sublimated by natural convection was observed and recorded.

b. Wind Tunnel Tests. Several standard models (for example, circular cone cylinders with a 4:1 fineness ratio, half-inch base diameters, and hemispherical nose cylinders) were tested at Mach 3 (atmospheric stagnation conditions) and their behavior was again observed and compared.

The behavior of all cast (recrystallized) models in both these standard tests was unsatisfactory. The surface developed pronounced nonuniformities, holes, and peaks, and soon became macroscopically rough. In wind-tunnel tests such surface roughness (in particular, surface depressions) tends to grow, sometimes resulting in serious changes in the flow field, visible as local shock structures. The sharp leading edge of the cone exhibited a clear tendency to break off in large chunks along prevalent crystalline surfaces; the large local changes thus produced in the shape of the leading edge subsequently propagated downstream in the form of deep axial grooves.

The scale of these disturbances, which seemed clearly related to the crystalline character of the model, was deemed unacceptably large for our purposes.

B. DIP CASTING (LAYER RECRYSTALLIZATION)

Experiences similar to those described above led other investigators to build up models by successively dipping a core in molten material. The initial external appearance of models produced by this method indicates a fairly homogeneous mass and a fine random-crystalline structure. The junction surfaces between successive layers are only faintly visible, and the material is completely opaque.

A number of models of different types were produced by this technique and tested. The crucial test, which led us to abandon this technique, consisted of alternately pouring and cooling liquid material in a cylindrical mold to build up a model composed of thin layers and then subjecting the model to the static oven test. Although the bond between the successive layers appeared to be good when the model was cold (for instance, models broken by shock and bending loads did not shear along the surfaces of the layers), the model disintegrated into a pile of elemental "dishes" after only a few minutes in the oven. This test was repeated several times, using different thicknesses of successive layers and different rates of cooling, with the same result.

It appears probable that the behavior of the layer interfaces is caused, at least in part, by trapped and absorbed air, which prevents a true interatomic bonding among crystals.

C. OPEN-AIR SINTERING (UNDEAERATED)

A sintering process was tried next. For this purpose, camphor was powdered and introduced into a cylindrical mold equipped with a piston. The mold and its contents were preheated in an isothermal bath and the powder was compressed at different rates to different final pressures (up to 40,000 psi). This is the process which is used to produce commercial products such as naphthalene moth balls.

When cold, sintered models are strong, devoid of visible crystalline structure, opaque, somewhat rough, but easily machinable. However,, their behavior under testing still seemed unsatisfactory.

Figure B-1 shows a model produced by this technique after 15 minutes in the static oven. The surface of the cylinder is partly covered with a loose, powder-like residue. The end cross section of the cylinder has not sublimated uniformly.

Figure B-2 shows selected Schlieren photographs of a test on a blunt (hemispherical) nose-cone cylinder produced by open-air sintering. This model exhibited from the start a band of granular material on the cylindrical afterbody. Such granular patches appeared occasionally in models produced by this method, either on the surface or within the mass of the material. They resembled a composite mass of small, independent crystals with voids. However, the crystals seemed larger than the initial size of the powder particles used.

During the test it soon became evident that the characteristics of the granular patches are entirely different from those of the remainder of the material. The patches appear clearly after three minutes, change little during most of the test (twenty-five minutes in the wind tunnel, Mach 3, atmospheric stagnation conditions), and finally break off.

The explanation of the observed phenomenon is not clear. Whatever aerothermal surface characteristics are responsible for the behavior of the granular patches, it is obvious that their occurrence on or beneath the surface is unacceptable for the study.

D. DEAERATED POWDER SINTERING

The disintegration of dip-cast models along the interlayer surfaces upon heating, and the appearance of the granular patches in sintered models, suggested that the difficulty may stem from the presence of a foreign gas (air) in the mass of camphor, both in interparticle voids and adsorbed on the surface.

On the basis of these considerations a vacuum-tight mold was built, equipped with a piston and containing ducts and grooves in its

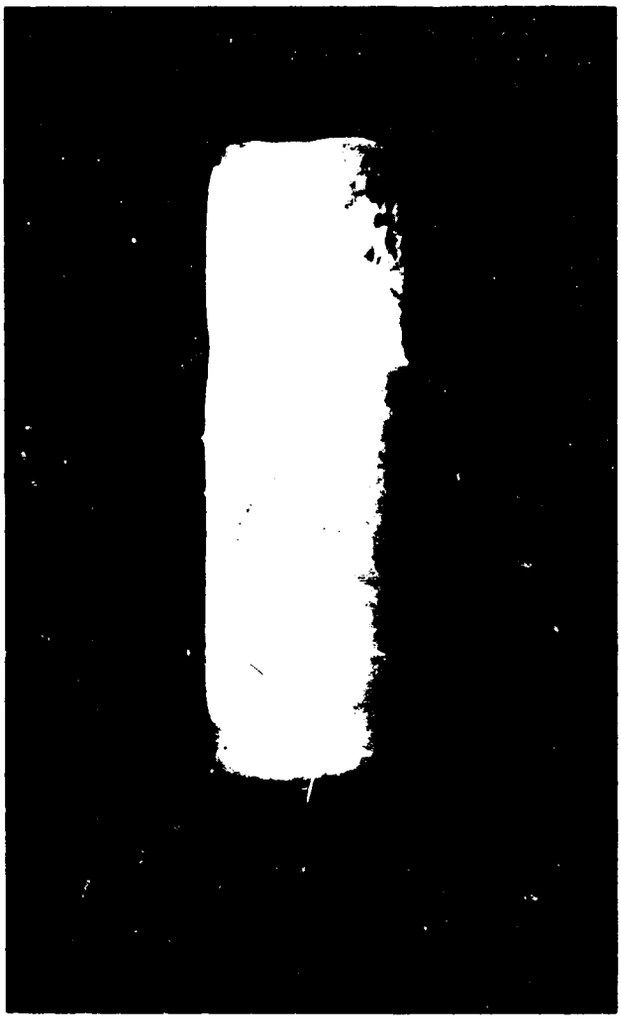

Fig. B-1—Sintered camphor model after 15 minutes in an oven at 150 °F (not pre-deaerated)

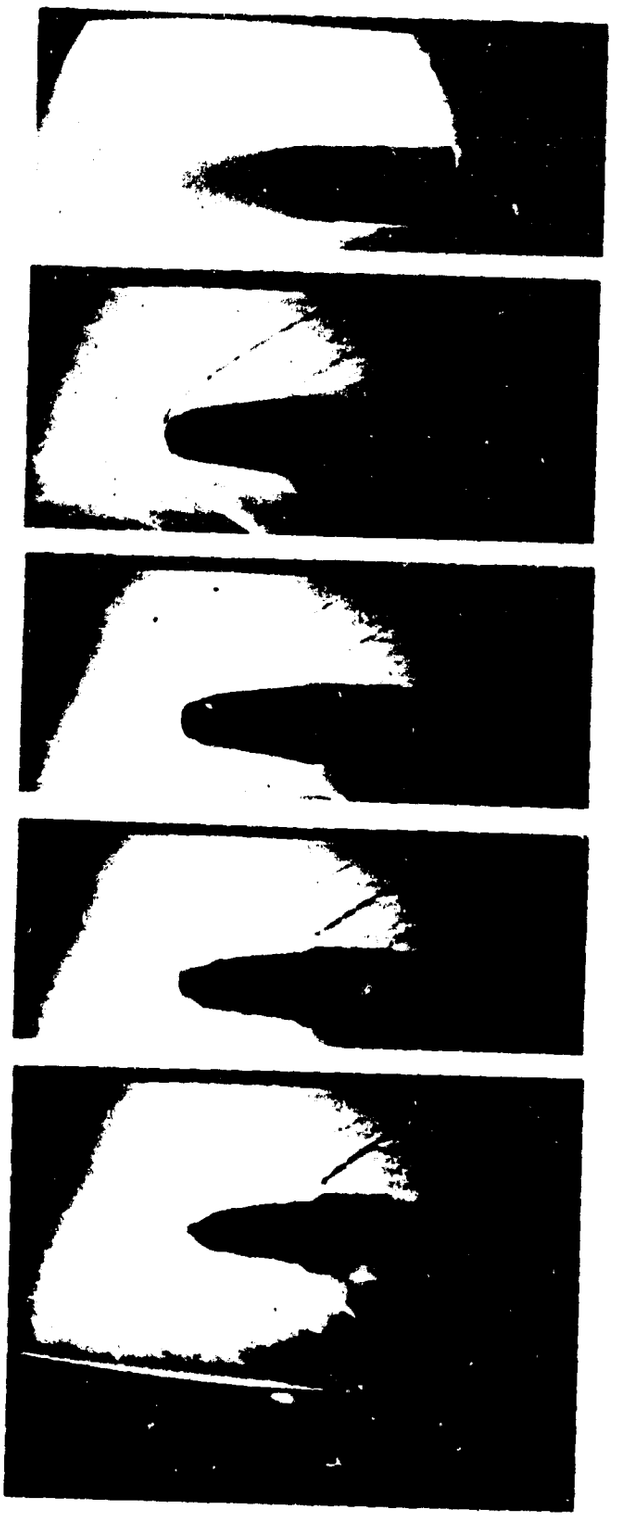

Fig. B-2—Sublimation of sintered (not deaerated) camphor hemisphere-cone-cylinder; M = 3, T_{STAG} = 79°F, Re ~ 100,000 per inch (note behavior of "granular" patch)

internal surface through which gas could be removed from the mold by pumping. [A second type of mold with two pistons (see Fig. B-3) was constructed later, for reasons described below.] The mold was then filled with powdered material, which was subjected to reduced pressure, typically for 10 to 15 minutes. Because the pressure was maintained below that of the triple point at the corresponding temperature, the material sublimated, expelling the air contained in the voids and adsorbed on the surface of the powder particles, and the gas was pumped from the mold. The piston was then disengaged and the powder was compressed.

The models fabricated by this procedure are absolutely homogeneous and smooth. One such model is shown in Fig. B-4 after 15 minutes in a static oven (compare with Fig. B-1). This photograph was chosen to demonstrate the two different types of material obtained during the vacuum-sintering experiments: (a) a clear, translucent mass and (b) a milky white, opaque mass. Both types behaved in the same fashion during all tests. However, the clear casting was judged intuitively preferable for aerodynamic studies.

The milkiness seems to be associated with the compression process; in the two-inch cylinder shown in Fig. B-4 it appeared at the end adjacent to the single piston, whereas the opposite end remained clear. Moreover, when one clear model was suddenly cooled to the temperature of dry ice it turned milky, suggesting that the milkiness is the result of microscopic faults and cracks produced in the cylinder by nonisotropic heat conduction and residual shears in the material.

As the result of these observations, and because the clear model was judged preferable, the two-piston mold shown in Fig. B-3 was fabricated. This design minimizes the travel of each piston, compressing the powder more uniformly and resulting in a uniformly clear cylinder.

A variety of combinations of temperature (room to 200°F), pressure (up to 40,000 psi), and rate of compression (including impact) was tried in the double-piston mold. Higher temperatures generally seem to induce plastic flow during compression (sometimes extruding the material through the vacuum passages), and produce axially nonuniform samples similar to those produced in the single-piston mold.

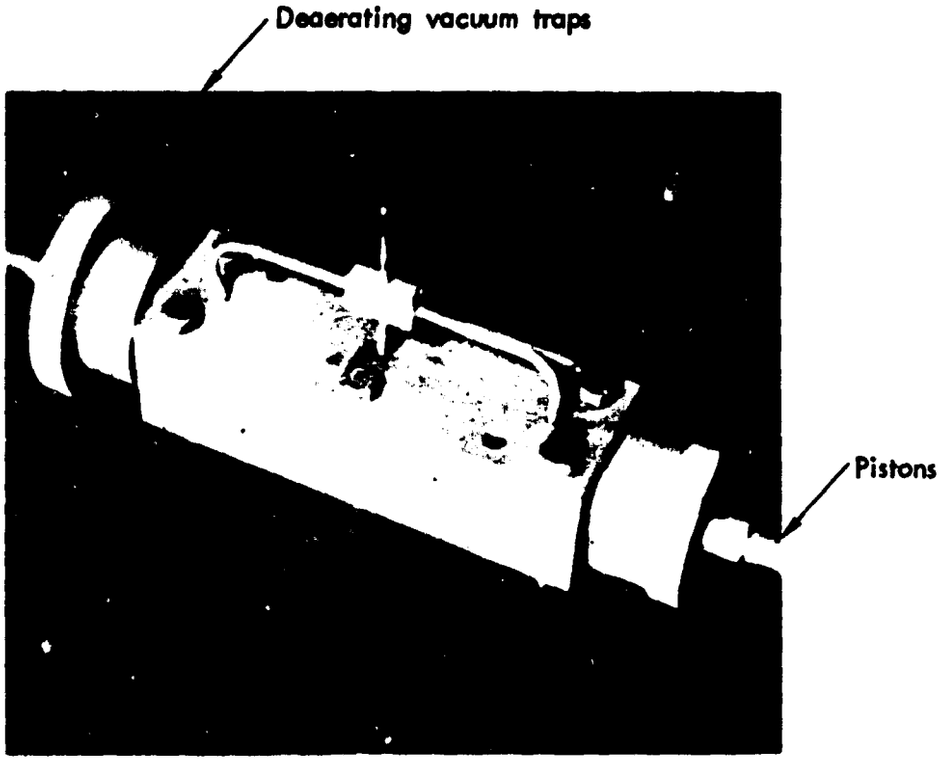

Fig. B-3—Two-piston mold for sintering camphor cylinders (1/2 in. diameter, 2 in. long), with provisions for deaerating prior to compression

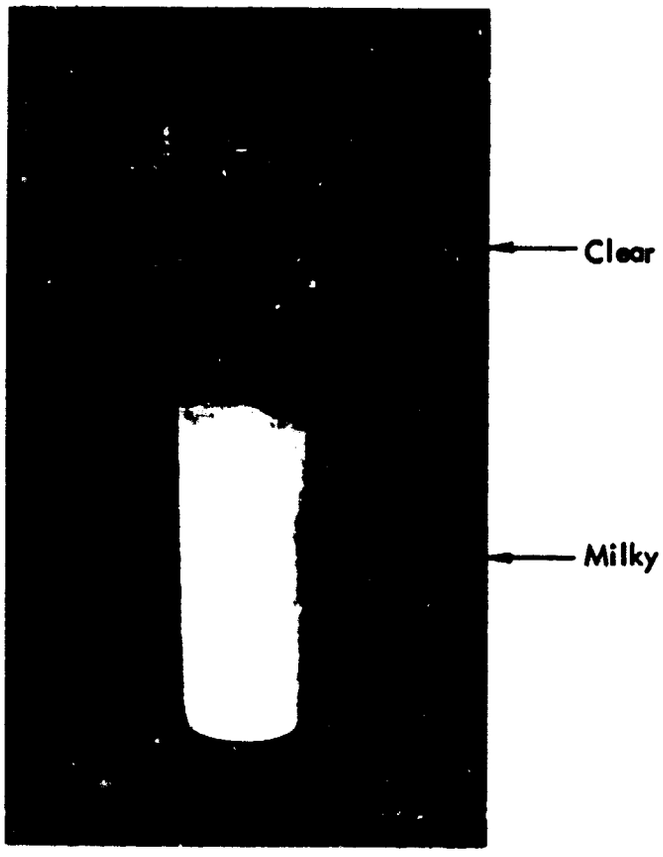

Fig. B-4—Deaerated, sintered camphor model after 15 minutes in an oven at 150°F (produced in single-piston mold)

Impact loading leads to milky samples. The simplest method appears to be the most satisfactory; it was found that reproducible, homogeneous, completely clear 2-inch cylinders can be produced by use of the double-piston mold (after deaeration of the material for 10 to 15 minutes) to apply pressures gradually for several seconds at room temperature, up to a maximum of 5000 psi. We believe that other shapes and sizes can also be produced satisfactorily, after perhaps minor adjustments in the design of the mold and in the compression technique.

REFERENCES

1. Canning, T. N., M. E. Tauber, and M. E. Wilkins, "Review of Recent Ballistic Range Boundary Layer Transition Work on Ablating Bodies at Ames," presented at Boundary Layer Transition Study Group, Aerospace Corporation, San Bernardino, California, July 11-12, 1967 (Summary in AIAA J., January 1968).

2. Wilkins, M. E., "Evidence of Surface Waves and Spreading of Turbulence on Ablating Models," AIAA J., Vol. 3, 1965, pp. 1963-1966.

3. Wilkins, M. E., and M. E. Tauber, "Boundary Layer Transition on Ablating Cones at Speeds up to 7 km/sec," AIAA J., Vol. 4, August 1966, pp. 1344-1348.

4. Canning, T. N., M. E. Wilkins, and M. E. Tauber, "Boundary Layer Phenomena Observed on the Ablated Surfaces of Cones Recovered After Flights at Speeds up to 7 km/sec," presented at AGARD Specialist Meeting of the Fluid Dynamics Panel, Colorado State University, Fort Collins, Colorado, May 1967.

5. Kubota, T., "Ablation with Ice Model at M = 5.8," ARS J., December 1960, pp. 1164-1169.

6. Weiss, R., Sublimation of a Hemisphere in Supersonic Flow, Massachusetts Institute of Technology, Naval Supersonic Laboratory Technical Report 391 (AF 49(638)245), July 1959.

7. Charwat, A. F., Preparation of Camphor Models for Wind-Tunnel Sublimation Studies: Preliminary Results on the Sublimation of a Pointed Cone, The RAND Corporation, P-2611, July 1962.

8. Sayano, S., Investigation of the Use of Low Temperature Materials for Studies of Ablation and Sublimation in Supersonic Flow, M.S. Thesis, Department of Engineering, U.C.L.A., October 1962.

9. Charwat, A. F., The Effect of Surface-Evaporation Kinetics on the Sublimation into a Boundary Layer, The RAND Corporation, RM-3291-PR; also in Intern. J. Heat Mass Trans., Vol. 8, March 1965, pp. 383-394.

10. Christensen, D., and R. Buhler, "On the Stable Shape of an Ablating Graphite Body," J. Aero. Sci., Vol. 26, No. 1, January 1959.

11. Gross, J. F., J. P. Hartnett, D. J. Masson, and C. Gazley, Jr., A Review of Binary Boundary Layer Characteristics, The RAND Corporation, RM-2516, June 1959.

12. van Driest, E. R., Investigation of Laminar Boundary Layer in Compressible Fluids Using the Crocco Method, NACA TN-2597, January 1952.

13. Lees, L., Convective Heat Transfer with Mass Addition on Chemical Reaction, 3rd AGARD Combustion and Propulsion Panel Colloquium, Pergamon Press, March 1958, pp. 451-498.

14. Boundary Layer Transition Study Group Meeting, Aerospace Report No. TR-0158 (S3816-63)-1, Vol. III, Paper 17, August 1967.

DOCUMENT CONTROL DATA

1 ORIGINATING ACTIVITY	2a. REPORT SECURITY CLASSIFICATION
THE RAND CORPORATION	UNCLASSIFIED
	2b. GROUP

3. REPORT TITLE

EXPLORATORY STUDIES ON THE SUBLIMATION OF SLENDER CAMPHOR AND NAPHTHALENE MODELS IN A SUPERSONIC WIND-TUNNEL

4. AUTHOR(S) (Last name, first name, initial)

Charwat, A. F.

5. REPORT DATE	6a. TOTAL No. OF PAGES	6b. No. OF REFS.
July 1968	73	14

7. CONTRACT OR GRANT No.	8. ORIGINATOR'S REPORT No.
DAHC15-67-C-0141	RM-5506-ARPA

9a. AVAILABILITY/LIMITATION NOTICES	9b. SPONSORING AGENCY
DDC-1	Advanced Research Projects Agency

10. ABSTRACT

A summary of a systematic study of the sintering of powdered camphor and naphthalene after deaeration under vacuum. It is shown that models machined out of stock prepared in this way have a shear strength twice that of cast models, are completely homogeneous, and are well suited to wind-tunnel experiments on the aerodynamics of subliming bodies. Exploratory tests on cones with flat and hemispherical noses and on several complex conical shapes featuring downstream and upstream facing steps, rectangular grooves, and shoulders are described. Emphasis is on the general evolution of their profiles, the sublimation history of the tips, and the occurrence of grooves, striations, and surface markings.

11. KEY WORDS

Aerodynamics
Ablation
Physics
Heat transfer
Thermodynamics
Materials
Chemistry
Fluid dynamics